HHS Public Access

Author manuscript

*Cell Rep*. Author manuscript; available in PMC 2022 May 17.

Published in final edited form as:

*Cell Rep*. 2022 April 12; 39(2): 110657. doi:10.1016/j.celrep.2022.110657.

# TNF-α sculpts a maturation process *in vivo* by pruning tolerogenic dendritic cells

**Courtney A. Iberg**[1,2,3], **Jessica Bourque**[1,3], **Ian Fallahee**[1], **Sungho Son**[1], **Daniel Hawiger**[1,4,*]

[1]Department of Molecular Microbiology and Immunology, Saint Louis University School of Medicine, St. Louis, MO, USA

[2]Present address: Department of Pathology and Immunology, Division of Immunobiology, Washington University School of Medicine, St. Louis, MO, USA

[3]These authors contributed equally

[4]Lead contact

## SUMMARY

It remains unclear how the pro-immunogenic maturation of conventional dendritic cells (cDCs) abrogates their tolerogenic functions. Here, we report that the loss of tolerogenic functions depends on the rapid death of BTLA$^{hi}$ cDC1s, which, in the steady state, are present in systemic peripheral lymphoid organs and promote tolerance that limits subsequent immune responses. A canonical inducer of maturation, lipopolysaccharide (LPS), initiates a burst of tumor necrosis factor alpha (TNF-α) production and the resultant acute death of BTLA$^{hi}$ cDC1s mediated by tumor necrosis factor receptor 1. The ablation of these individual tolerogenic cDCs is amplified by TNF-α produced by neighboring cells. This loss of tolerogenic cDCs is transient, accentuating the restoration of homeostatic conditions through biological turnover of cDCs *in vivo*. Therefore, our results reveal that the abrogation of tolerogenic functions during an acute immunogenic maturation depends on an ablation of the tolerogenic cDC population, resulting in a dynamic remodeling of the cDC functional landscape.

## In brief

Here, Iberg et al. reveal that the loss of tolerogenic functions under the pro-inflammatory conditions induced by LPS depends on the rapid physical elimination of inherently tolerogenic cDCs from peripheral lymphoid organs. This process depends on a burst of TNF-α production and a resultant acute and specific TNFR1-mediated death.'



*Correspondence: daniel.hawiger@health.slu.edu.

AUTHOR CONTRIBUTIONS

Conceptualization, C.A.I., J.B., and D.H.; methodology, C.A.I., J.B., and D.H.; investigation, C.A.I., J.B., and S.S.; resources, I.F.; formal analysis, J.B.; visualization, J.B.; writing – original draft, J.B. and D.H.; writing – review & editing, all authors; supervision, D.H.; funding acquisition, D.H.

DECLARATION OF INTERESTS

The authors declare no competing interests.

SUPPLEMENTAL INFORMATION

Supplemental information can be found online at https://doi.org/10.1016/j.celrep.2022.110657.

## Graphical Abstract

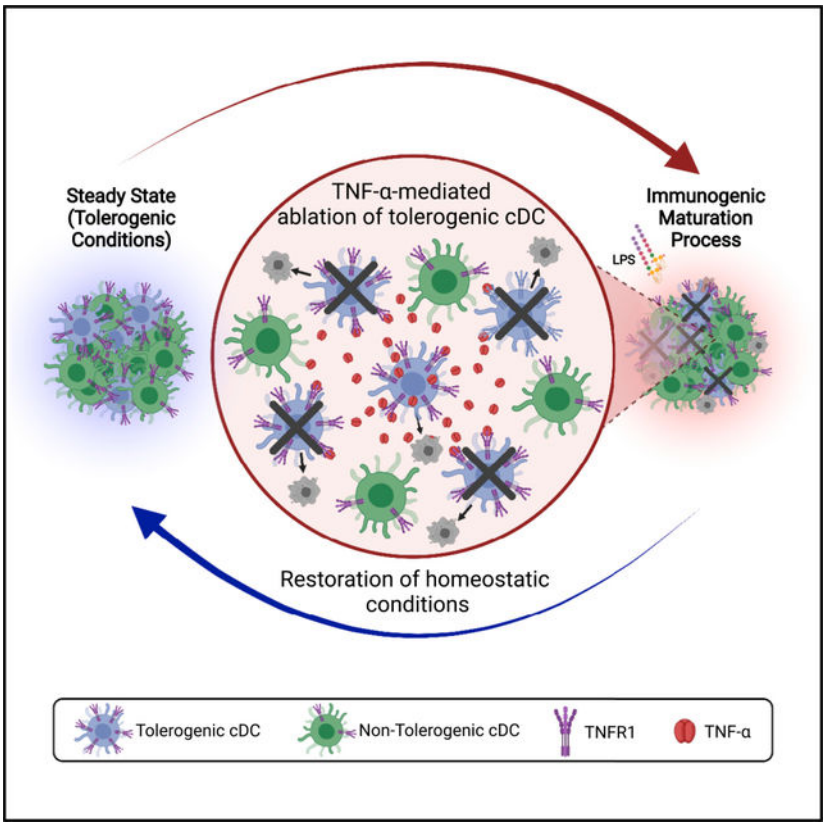


## INTRODUCTION

The absence of specific pro-inflammatory signals, referred to as the steady state, is conducive to induction and maintenance of peripheral T cell tolerance, while the disturbance of steady-state conditions by pro-inflammatory stimuli generally results in a change from tolerogenic to immunogenic outcomes of conventional dendritic cell (cDC) and T cell interactions (Cabeza-Cabrerizo et al., 2021; Dalod et al., 2014; Iberg et al., 2017; Iwasaki and Medzhitov, 2015; Mellman, 2013; Steinman et al., 2003a). The recognition of pathogen-associated molecular patterns (PAMPs) through the corresponding pattern recognition receptors (PRRs) triggers activation of cDCs in a process referred to as maturation that results in the acquisition of specific immune functions (Dalod et al., 2014; Iwasaki and Medzhitov, 2015; Mellman, 2013; Steinman, 2012; Steinman et al., 2003a). The archetypical concept of maturation was established early by studying the impact of a canonical PAMP, lipopolysaccharide (LPS), on T cell priming (Cabeza-Cabrerizo et al., 2021; De Smedt et al., 1996). Subsequent studies found that maturation induced by LPS and other PAMPs enhances in individual cell functions of the inflammasome and increases the expression of major histocompatibility complexes (MHCs), multiple costimulatory ligands, cytokines, and other molecules that collectively enable pro-immunogenic effector T cell priming (Dalod et al., 2014; Fitzgerald and Kagan, 2020; Mellman, 2013). After mature cDCs complete the process of T cell priming, their death may be critical to avoid excessive immune activation

(Chen et al., 2006; Stranges et al., 2007). Further, long-term sequelae of infections include remodeling of the cDC population (Fonseca et al., 2015). However, cDCs also may undergo a programmed cell death soon after initiation of the maturation process (De Trez et al., 2005; Zanoni et al., 2009, 2016). This is consistent with other studies that observed an LPS-induced death and reduced numbers of cDCs, especially among the CD8 $\alpha^+$ subset, usually attributing it to mechanisms regulating T cell priming while also serving as a potential source of antigenic materials (De Smedt et al., 1996; Fuertes Marraco et al., 2011; Qiu et al., 2009; Sundquist and Wick, 2009; Xu et al., 2017). Further, in a model of sepsis, functions of glucocorticoids regulated the loss of CD8$\alpha^+$ cDCs (Li et al., 2015). However, more recent studies uncovered relevant molecular mechanisms that specifically prevent the pyroptotic death of maturing cDCs, therefore directly preserving their immune functions (McDaniel et al., 2020; Zhivaki et al., 2020).

In addition to stimulating immune functions, some microbial as well as endogenous, including tumor-associated, maturation stimuli also induce specific tolerogenic properties in cDCs (Anderson et al., 2009; Harimoto et al., 2013; Iberg and Hawiger, 2020; Maier et al., 2020; Wang et al., 2019; Zhou et al., 2014). Various types of cDCs with such tolerogenic functions, especially those that migrate to draining lymph nodes (LNs), have important roles for maintaining homeostasis at anatomical barriers exposed to the commensal microbiota and other environmental cues (Arpaia et al., 2013; Cummings et al., 2016; Esterhazy et al., 2019; Guilliams et al., 2010; Iberg and Hawiger, 2020; Kashem et al., 2017; Manicassamy and Pulendran, 2011; Miller et al., 2012; Russler-Germain et al., 2021; Vitali et al., 2012). In contrast to cDCs at anatomical barriers, systemic cDCs are present throughout the peripheral lymphoid organs and constantly survey local and circulating antigens derived from parenchymal, interstitial, and other non-barrier tissues. Further, the systemic cDCs can present antigens from pathogens during infections as well as those introduced by intramuscular vaccinations (Bourque and Hawiger, 2022). However, most systemic cDCs do not remain as immunologically inert bystanders in the steady state and are instead functionally competent *in vivo*, possibly in response to yet incompletely identified molecular ligands constitutively present in the steady state as well as other specific mechanisms operating intrinsically in cDCs under homeostatic conditions (Ardouin et al., 2016; Baratin et al., 2015; Dalod et al., 2014; Hammer and Ma, 2013; Iberg et al., 2017; Jiang et al., 2007; Manh et al., 2013; Vander Lugt et al., 2017). Such immunologically competent cDCs are responsible for the various effector and regulatory outcomes of T cell activation observed in the steady state (Bourque and Hawiger, 2022; Opejin et al., 2020).

The dominant forms of peripheral tolerance dependent on *de novo* induced peripheral regulatory T (pTreg) cells limit effector immune responses and crucially complement immunological tolerance first initiated in the thymus (Iberg et al., 2017; Jones and Hawiger, 2017; Jones et al., 2015). The induction of such systemic pTreg cells is efficiently mediated in the steady state by cDCs with inherent tolerogenic functions that belong to the Batf3-dependent, XCR1$^+$ type 1 subset (cDC1), corresponding to previously defined DEC-205$^+$CD8$\alpha^+$ cDCs (Guilliams et al., 2014; Iberg and Hawiger, 2020; Iberg et al., 2017; Steinman et al., 2003b). These tolerogenic cDC1s are further distinguished by their high expression of B- and T-lymphocyte associated/attenuator (BTLA) (Jones et al., 2016). In concert with some other mechanisms present in these cDC1s, BTLA promotes an efficient

induction of pTreg cells in response to systemic antigens (Bourque and Hawiger, 2018; Iberg et al., 2017; Jones et al., 2016; Yin et al., 2021). The BTLA$^{hi}$ cDC1s are present in peripheral lymphoid organs, including spleen and LNs, and are therefore ideally positioned to present to T cells self-antigens, including those obtained from apoptotic materials (Albert et al., 1998; Belz et al., 2002; Eisenbarth, 2019; Iberg and Hawiger, 2020; Iyoda et al., 2002; Steinman et al., 2003b). Overall, the tolerance promoted in the steady state blocks subsequent immune responses induced by a pro-immunogenic maturation of cDCs. Crucially, however, it remains unclear how the functional re-programming during a pro-immunogenic maturation induced by PAMPs such as LPS abrogates tolerogenic functions of cDCs.

We now found that, instead of altering the functionality of individual tolerogenic cDCs, pro-immunogenic signals transiently remove the entire population of specialized tolerogenic cDCs. Upon induction of pro-inflammatory conditions *in vivo*, tolerogenic BTLA$^{hi}$ cDC1s are specifically ablated through the mechanisms of programmed cell death mediated by the functions of tumor necrosis factor alpha (TNF-α) and tumor necrosis factor receptor 1 (TNFR1), resulting in an abrogation of the specific *de novo* conversion of pTreg cells. Our findings further revealed that the production of TNF-α by neighboring cells potentiates this ablation of BTLA$^{hi}$ cDC1s, therefore amplifying the initial LPS-initiated signals. Consistent with the established rapid turnover and replenishment of cDCs *in vivo* (Kamath et al., 2000; Liu et al., 2007), the BTLA$^{hi}$ cDC1 tolerogenic population is restored within a few days. Overall, these findings expand the concept of immunogenic activation and maturation to crucially include a dynamic reshaping of the cDC population and ablation of tolerogenic cDCs. By revealing the role of TNF-α and TNFR1 in mediating the loss of tolerogenic cDCs, these results also clarify functions of TNF-α during the maturation process. Further, by elucidating the dynamic cycle of a transient loss and subsequent restoration of tolerogenic cDCs, they help to clarify the biological role of the constant turnover of cDCs *in vivo*.

## RESULTS

### Tolerogenic cDCs are ablated under pro-inflammatory conditions

We applied the currently established approach for identification of XCR1$^{+}$ cDC1s and CD172a$^{+}$ cDC2s (Guilliams et al., 2016) to rigorously analyze splenic cDCs following administration of LPS *in vivo* (Figure S1A). Within 1 day after administration of LPS, the proportion of XCR1$^{+}$ cDC1s among cDCs was reduced by about 60%–70%, whereas the relative proportion of cDC2s among cDCs correspondingly increased (Figures 1A–1C). A terminal deoxynucleotidyl transferase deoxyuridine triphosphate (dUTP) nick end labeling (TUNEL) assay confirmed the death of cDC1s (Figure 1D). Consistent with their multifaceted functions in priming and regulating immune responses, cDC1s are heterogeneous (Durai and Murphy, 2016). The BTLA$^{hi}$ cDC1s are characterized by the highest expression of BTLA among all cDCs (Figure S1B) and have established tolerogenic functions (Jones et al., 2016). The BTLA$^{hi}$ cDC1s were disproportionally decreased by about 3-fold among the splenic cDC1s that remained 24 h after administration of LPS (Figure 1E). In contrast, the BTLA$^{lo}$ cDC1s and cDC2s increased expression of

costimulatory molecules, such as CD86, consistent with their maturation (Figures S1C and S1D). We next confirmed the almost complete loss of BTLA$^{hi}$ cDC1s by measuring their proportion among all cDCs as well as leukocytes and by counting the absolute numbers of splenic BTLA$^{hi}$ cDC1s, whereas the number of total splenocytes remained similar in mice that were treated with either PBS or LPS (Figures 1F–1I and S1E). Overall, we established that the relevant loss of BTLA$^{hi}$ cDC1s could be comparably represented as a reduced fraction of either total cDCs or total leukocytes as well as by the absolute numbers (Figure 1J). Importantly, a similar loss of BTLA$^{hi}$ cDC1s was observed in response to different doses (1–10 μg/mouse) of LPS (Figure 1K).

In *Batf3*$^{-/-}$ mice that lack most splenic cDC1s, the *de novo* conversion of pTreg cells is reduced (Hildner et al., 2008; Jones et al., 2016; Tussiwand et al., 2012). Consistent with these results, we found a near absence of splenic BTLA$^{hi}$ cDC1s in *Batf3*$^{-/-}$ mice and a corresponding lack of induction of antigen-specific pTreg cells following the specific *in vivo* delivery of cognate antigen (Figures S1F–S1H). As expected, and in agreement with a general abrogation of tolerogenic outcomes of cDCs and T cell interactions under acutely induced pro-inflammatory conditions, we observed a comparable absence of such *de novo* induced pTreg cells in the *Batf3*$^{+/+}$ (wild-type [WT]) mice in which BTLA$^{hi}$ cDC1s were ablated by LPS (Figure 1L). Overall, we conclude that, consistent with their established general pro-immunogenic effects, inflammatory conditions acutely induced by LPS result in the loss of tolerogenic BTLA$^{hi}$ cDC1s.

## BTLA$^{hi}$ cDC1s are ablated in *trans*

In addition to its roles in promoting pTreg cell conversion through ligand-receptor interactions with herpesvirus entry mediator (HVEM) expressed by T cells (Bourque and Hawiger, 2019; Henderson et al., 2015; Jones et al., 2016), BTLA also has cell-autonomous functions (Kobayashi et al., 2013; Murphy and Murphy, 2010; Shui et al., 2011). To test the possible impact of such functions on the loss of BTLA$^{hi}$ cDC1s, we analyzed cDCs in *Btla*$^{-/-}$ mice and found a similar decrease in cDC1s in response to LPS, regardless of the presence or absence of BTLA (Figure S2A). Further, the ablation of BTLA$^{hi}$ cDC1s was independent of Fas and type I interferon receptor (IFNAR), which are involved in mediating certain types of cell death and cDC homeostasis (Fuertes Marraco et al., 2011; Mattei et al., 2009; Schaupp et al., 2020; Stranges et al., 2007; Figures S2B and S2C). The effects of LPS are signaled through several molecular pathways (Fitzgerald and Kagan, 2020). Toll-like receptor 4 (TLR4) is a canonical LPS receptor that is expressed by cDC1s (Edwards et al., 2003), and the loss of BTLA$^{hi}$ cDC1s following LPS administration was completely dependent on the presence of TLR4 (Figure 2A). To further clarify the mechanisms resulting in the loss of BTLA$^{hi}$ cDC1s, we confirmed the roles of pathways known to mediate cell death. Receptor-interacting serine and threonine-protein kinase 3 (RIPK3), caspase 3, and caspase 8 are established executers of programmed death pathways (Kolb et al., 2017; Nagata and Tanaka, 2017). In the steady state, the proportion of BTLA$^{hi}$ cDC1s among cDCs was unaffected by the absence of RIPK3, caspase 3, and caspase 8 (Figures S2D and S2E). Supporting the functions of these programmed death pathways in mediating the ablation of BTLA$^{hi}$ cDC1s, this population was only moderately reduced in the *Ripk3*$^{-/-}$*Casp3*$^{-/-}$*Casp8*$^{\Delta CD11c}$ mice in response to LPS, remaining at about 50%

of its steady-state baseline (Figure 2B). The relationship between TLR4-mediated signals and programmed death mechanisms is complex, and LPS can affect functions of multiple hematopoietic and non-hematopoietic cell populations (Fitzgerald and Kagan, 2020). In agreement with autonomous functions of TLR4 in hematopoietic cells, LPS-induced ablation was prevented in BTLA$^{hi}$ cDC1s developing from the *Tlr4*$^{-/-}$ bone marrow (BM) that reconstituted chimera mice similarly to *Tlr4*$^{+/+}$ BM (Figures 2C and S2F). A conditional deletion of *Tlr4* in macrophages or B cells did not prevent a loss of BTLA$^{hi}$ cDC1s in response to LPS (Figures S2G and S2H). In contrast, a specific deletion of *Tlr4* using *Itgax*-Cre that deletes most efficiently in CD11c$^{+}$ cDCs (Abram et al., 2014; Melillo et al., 2010; Figure S2I) rescued such a loss of BTLA$^{hi}$ cDC1s (Figure 2D), revealing the relevant mechanisms to be dependent on the expression of TLR4 specifically in CD11c$^{+}$ cDCs. These specific TLR4-mediated functions were also dependent on signaling through myeloid differentiation primary response protein MyD88 (MyD88) and Toll/interleukin-1 (IL-1) receptor (TIR)-domain-containing, adapter-inducing interferon-β (TRIF) (Figure 2E). To distinguish whether the TLR4-dependent death and ablation of BTLA$^{hi}$ cDC1s proceeded cell autonomously in the individual cDCs or whether such ablation depended on additional extrinsic factors, we constructed *Trif*$^{+/+}$*Myd88*$^{+/+}$:*Trif*$^{-/-}$*Myd88*$^{\Delta CD11c}$ mixed BM chimeras and confirmed an equal reconstitution of the cDC populations (Figures 2F and S2J). As expected, we observed a specific loss of the *Trif*$^{+/+}$*Myd88*$^{+/+}$ BTLA$^{hi}$ cDC1s in response to LPS. However, unexpectedly, we found a similar ablation of the *Trif*$^{-/-}$*Myd88*$^{\Delta CD11c}$ BTLA$^{hi}$ cDC1s in these LPS-treated mixed BM chimeras (Figure 2F). This suggested that the ablation of BTLA$^{hi}$ cDC1s is mediated indirectly (in *trans*) within the cDC population. Further consistent with such an indirect mechanism, we observed a comparable ablation of both *Tlr4*$^{-/-}$ and *Tlr4*$^{+/+}$ BTLA$^{hi}$ cDC1 populations within the equally reconstituted *Tlr4*$^{-/-}$:*Tlr4*$^{+/+}$ mixed BM chimeras treated with LPS (Figures 2G and S2K). We conclude that the initial TLR4-dependent sensing of LPS by cDCs mediates a secondary, TLR4-independent death and ablation of BTLA$^{hi}$ cDC1s.

## Rapid production of TNF-α mediates and amplifies the ablation of BTLA$^{hi}$ cDC1s

To further characterize the ablation of BTLA$^{hi}$ cDC1s, we examined the cDC population at multiple time points after administration of different doses of LPS. We observed an initial, about 25% decrease of BTLA$^{hi}$ cDC1s already by 3 h, a 50% reduction of this population by 6 h, and an almost complete ablation of the BTLA$^{hi}$ cDC1s within 24 h (Figures 3A and S3A). Such an early onset of ablation suggested a role for a rapidly produced mediator. TNF-α, which is encoded by an immediate-early gene, is produced following exposure to specific signals (Falvo et al., 2010). Production of TNF-α is associated with a process of cDC activation (Kaisho et al., 2001). Further, TNF-α is well established to mediate programmed cell death (Wajant and Siegmund, 2019). We found that TNF-α production by cDCs peaked about 1 h after LPS administration, and cDC1s were the main producers of TNF-α with about 60% of cDC1s producing TNF-α at the peak production point, whereas fewer than 10% of cDC2s produced TNF-α (Figures 3B–3E and S3B). This TNF-α production was dependent on the expression of TLR4 in cDCs and the corresponding functions of MyD88/TRIF but under these conditions did not require functions of other signaling pathways involving receptors such as IFNAR (Figures 3F, 3G, and S3C–S3F). Among cDC1s, the major producers of TNF-α were BTLA$^{hi}$ cDC1s, with about 70%

of these cells becoming positive for TNF-α, whereas only 30%–40% of BTLA$^{lo}$ cDC1s produced TNF-α (Figure 3H). To test directly whether such acutely produced TNF-α promotes ablation of BTLA$^{hi}$ cDC1s, we pre-treated mice with an anti-TNF-α blocking antibody before administering LPS. LPS-treated mice that received anti-TNF-α blocking antibody had five to eight times more BTLA$^{hi}$ cDC1s among total cDCs as compared with LPS-treated mice without such an anti-TNF-α blockade, indicating a key role for TNF-α in mediating the ablation of BTLA$^{hi}$ cDC1s (Figure 3I). To elucidate whether TNF-α was required to mediate the ablation of BTLA$^{hi}$ cDC1s in *trans* in the absence of other signals that could be directly induced by LPS in such responding cells, we tested the impact of blocking TNF-α in the *Tlr4*$^{-/-}$:*Tlr4*$^{+/+}$ mixed BM chimeras. As expected, the administration of LPS resulted in a loss of *Tlr4*$^{-/-}$ BTLA$^{hi}$ cDC1s in the *Tlr4*$^{-/-}$:*Tlr4*$^{+/+}$ mixed BM chimeras treated with an isotype control antibody. However, blocking of TNF-α reversed the effects of LPS, completely preventing the loss of these BTLA$^{hi}$ cDC1s (Figure 3J). Therefore, under pro-inflammatory conditions, TNF-α propagates the ablation of BTLA$^{hi}$ cDC1s independently of specific innate signaling in these cells.

Some non-specific signals produced under LPS-induced pro-inflammatory conditions might indirectly facilitate the TNF-α-mediated ablation of BTLA$^{hi}$ cDC1s. Therefore, to test directly whether TNF-α is sufficient to mediate the ablation of BTLA$^{hi}$ cDC1s, we administered purified recombinant TNF-α protein *in vivo* in the absence of an exposure to LPS. In the absence of LPS treatment, administration of TNF-α induced a robust loss of BTLA$^{hi}$ cDC1s (Figures 3K and 3L). Therefore, we conclude that TNF-α is sufficient to mediate ablation of BTLA$^{hi}$ cDC1s even in the absence of an innate stimulus. This result also suggested that the production of TNF-α in response to LPS can amplify the ablation of BTLA$^{hi}$ cDC1s when the innate stimulus is available only to a minor portion of cells *in vivo*. To clarify this, we used mixed BM chimeras with different ratios of *Tlr4*$^{-/-}$:*Tlr4*$^{+/+}$ cDCs (Figure 3M). Upon administration of LPS in these chimeras, we observed a robust ablation of *Tlr4*$^{-/-}$ BTLA$^{hi}$ cDC1s, even when they outnumbered their LPS-responsive counterparts by 4:1 (Figure 3M). Overall, we conclude that this induced production of TNF-α amplifies the ablation of individual BTLA$^{hi}$ cDC1s independently of a direct sensing by such cells of the original innate trigger of the pro-inflammatory maturation process.

## TNF-α-dependent ablation of BTLA$^{hi}$(CCR7$^{lo}$) cDC1s throughout peripheral lymphoid organs

CCR7 governs migration of cDCs; therefore, CCR7$^{hi}$ cDCs are considered to have migratory properties, whereas CCR7$^{lo}$ cDCs reside in the lymphoid organs (Ohl et al., 2004). We found almost all splenic BTLA$^{hi}$ cDC1s to have low expression of CCR7, and such BTLA$^{hi}$(CCR7$^{lo}$) cDC1s constituted the main population of splenic cDC1s in the steady state (Figure S4A). This is consistent with BTLA being a selective marker of tolerogenic cDCs in the lymphoid organs independently of other markers' expression (Jones et al., 2016). In agreement with their ablation in response to LPS, the BTLA$^{hi}$CCR7$^{lo}$ cDC1 population was decreased in the absence of a corresponding increase of a proportion of CCR7-expressing cDC1s (Figures 4A and S4B). Similar to their splenic counterparts, the BTLA$^{hi}$ cDC1s present in LNs are also CCR7$^{lo}$, but these BTLA$^{hi}$CCR7$^{lo}$ cDC1s constitute only a minor population among the LN cDC1s in the steady state (Figures S4C and

S4D). Nevertheless, treatment with LPS severely reduced this lymphoid BTLA$^{hi}$CCR7$^{lo}$ cDC1 population, underscoring a curtailed induction of pTreg cells in LNs under the pro-inflammatory conditions following administration of LPS (Figures 4B–4D). To confirm the key roles of TNF-α in mediating the deletion of BTLA$^{hi}$CCR7$^{lo}$ cDC1s independently of innate pro-inflammatory intrinsic signaling in these cells, we used *Tlr4*$^{-/-}$:*Tlr4*$^{+/+}$ mixed BM chimeras. We found that, similar to splenic BTLA$^{hi}$CCR7$^{lo}$ cDC1s (Figure S4E), blocking the TNF-α produced in response to LPS restored the numbers of *Tlr4*$^{-/-}$ BTLA$^{hi}$CCR7$^{lo}$ cDC1s in the LNs from the *Tlr4*$^{-/-}$:*Tlr4*$^{+/+}$ mixed BM chimeras (Figure 4E). To further ascertain the specific impact of TNF-α on BTLA$^{hi}$CCR7$^{lo}$ cDC1s independently of the conditions induced by an innate pro-inflammatory stimulus, we administered purified recombinant TNF-α protein *in vivo* in the absence of an exposure to LPS, similar to what we did in Figures 3K and 3L. Administration of TNF-α in the absence of LPS treatment specifically reduced the BTLA$^{hi}$CCR7$^{lo}$ population without affecting the proportions of other cDC populations present within LNs (Figures 4F, S4F, and S4G). Overall, we conclude that, upon acute induction of pro-inflammatory conditions, TNF-α promotes the loss of tolerogenic BTLA$^{hi}$(CCR7$^{lo}$) cDC1s in peripheral lymphoid organs.

## TNFR1 orchestrates the ablation of tolerogenic BTLA$^{hi}$ cDC1s

The cytotoxic effects of TNF-α in various types of cells are crucially mediated by TNFR1, also known as TNF receptor superfamily member 1A (TNFRSF1A) (Wajant and Siegmund, 2019). Consistent with the specific impact of TNF-α on BTLA$^{hi}$ cDC1s, this population exhibited the highest expression of TNFR1 among all other splenic cDCs in the steady state (Figures 5A and 5B). Also, the corresponding BTLA$^{hi}$CCR7$^{lo}$ population in LNs had a similar high expression of TNFR1, consistent with its sensitivity to TNF-α-mediated ablation (Figure S5A). To directly examine the role of TNFR1 in mediating the ablation of the BTLA$^{hi}$ cDC1s under pro-inflammatory conditions, we constructed *Tlr4*$^{-/-}$ *Tnfrsf1a*$^{-/-}$:*Tlr4*$^{+/+}$ *Tnfrsf1a*$^{+/+}$ and *Tlr4*$^{-/-}$ *Tnfrsf1a*$^{+/+}$:*Tlr4*$^{+/+}$ *Tnfrsf1a*$^{+/+}$ BM chimeras and confirmed the expected equal ratios of the correspondingly reconstituted cDCs both in spleens and LNs (Figures S5B and S5C). The absence of TNFR1 did not alter the proportions of BTLA$^{hi}$ cDC1s in these chimeras in the steady state (Figures 5D and 5E). However, whereas *Tlr4*$^{-/-}$ *Tnfrsf1a*$^{+/+}$ BTLA$^{hi}$ cDC1s were ablated in *trans* as expected, the ablation of the splenic *Tlr4*$^{-/-}$ *Tnfrsf1a*$^{-/-}$ BTLA$^{hi}$ cDC1s was completely prevented under the LPS-induced pro-inflammatory conditions (Figure 5D). Similarly, we observed a comparable lack of ablation of the *Tlr4*$^{-/-}$ *Tnfrsf1a*$^{-/-}$ BTLA$^{hi}$CCR7$^{lo}$ cDC1 population in LNs (Figure 5E). To clarify the impact of TNFR1-mediated effects on the tolerogenic functions of BTLA$^{hi}$ cDC1s, we examined the *de novo* conversion of pTreg cells in response to a specific antigen. In mice with unaltered responsiveness to LPS and TNF-α, the administration of LPS results in ablation of BTLA$^{hi}$(CCR7$^{lo}$) cDC1s and prevents pTreg cell formation as described above. In contrast, such pTreg cells could still be formed in both spleens and LNs by a small portion of *Tlr4*$^{-/-}$ *Tnfrsf1a*$^{-/-}$ BTLA$^{hi}$(CCR7$^{lo}$) cDC1s whose loss was prevented by their inability to respond to both the original innate stimulus as well as the ablation-amplifying signals mediated by TNF-α (Figures 5F–5H). Overall, we conclude that the abrogation of specific tolerogenic functions under acutely induced pro-inflammatory conditions proceeds through a physical deletion of a specialized cDC population that is amplified by TNFR1-dependent signals.

### A return to the homeostatic baseline by BTLA$^{hi}$ cDC1s

A prolonged absence of tolerogenic BTLA$^{hi}$(CCR7$^{lo}$) cDC1s and their functions could lead to an aberrant immuno-activation. Therefore, we extended our analysis of the populations of cDCs to later time points following the administration of different doses of LPS. The population of splenic BTLA$^{hi}$ cDC1s remained depressed for about 3 days (Figures 6A and S6A). An overall similar kinetic was also observed in the case of the relevant BTLA$^{hi}$CCR7$^{lo}$ cDC1 population in the LNs (Figure S6B). However, by 6 days after the initial exposure to LPS, the BTLA$^{hi}$ cDC1 population rebounded, and within about 12 days, it fully stabilized at its initial baseline (Figures 6A, 6B, and S6A–S6C). Therefore, the loss of tolerogenic BTLA$^{hi}$ cDC1s following the acute pro-inflammatory stimulus is transient, accentuating the constant biological turnover of cDCs *in vivo* from their BM precursors (Kamath et al., 2000; Liu et al., 2007). Further stressing this established compensatory replenishment of cDCs and a return to homeostatic conditions, the expression of TNFR1 in the newly replenished BTLA$^{hi}$ cDC1 population resembled that of the original population prior to the LPS exposure (Figures 6C and 6D). Consistent with a resetting of the sensitivity to the innate stimulus, the newly replenished BTLA$^{hi}$ cDC1 population could be ablated by a subsequent challenge with LPS (Figure 6E). Overall, we conclude that, following the ablation of tolerogenic BTLA$^{hi}$ cDC1s under pro-inflammatory conditions, the return to homeostatic conditions involves a re-establishment of this crucial population in the lymphoid organs and resetting their ability to respond to subsequent pro-inflammatory challenges.

## DISCUSSION

The pro-immunogenic maturation of cDCs abrogates their tolerogenic functions, but how this happened was unclear (Cabeza-Cabrerizo et al., 2021; Dalod et al., 2014; Iberg et al., 2017; Iwasaki and Medzhitov, 2015; Mellman, 2013; Steinman et al., 2003a). Our studies now expand the concept of the maturation of cDCs resulting from the disturbance of steady-state conditions by the introduction of PAMPs, such as LPS, as a process that crucially involves dynamic changes that reshape the composition of the cDC population. We revealed that the inherently tolerogenic cDCs are physically deleted from the peripheral lymphoid organs at the onset of the pro-inflammatory conditions induced by LPS. Therefore, maturation of cDCs emerges as a two-pronged process during which immunogenic activation of some cDCs is accompanied by a rapid ablation of the inherently tolerogenic cDCs to prevent *de novo* induction of pTreg cells. Further, and accentuating the dynamic role of biological turnover of cDCs *in vivo*, the loss of tolerogenic cDCs is transient, therefore avoiding potential long-term risks due to insufficient immunoregulation.

Our results clarify the functions of TNF-α as a key regulator of the fate of tolerogenic cDCs. BMDCs or monocyte-derived DCs (moDCs) cultured in vitro can acquire tolerogenic therapeutic potentials that could possibly be enhanced by TNF-α (Iberg and Hawiger, 2020; Menges et al., 2002; Zhou et al., 2014). However, despite potential translational significance, these results offer only limited insights into the biological characteristics of cDCs found *in vivo* because the BMDCs differ substantially from endogenous cDCs (Helft et al., 2015). By focusing on bona fide cDCs found *in vivo*, we instead revealed that, during LPS-induced

maturation, TNF-α mediates the death of BTLA$^{hi}$ cDC1s, resulting in a loss of tolerogenic functions. These effects depend on the TNF-α produced *in vivo* and can be prevented by a specific blockade of TNF-α. Consistent with such effects of TNF-α, BTLA$^{hi}$ cDC1s are key producers of TNF-α in response to an innate signal. Both the production of TNF-α and the ablation of BTLA$^{hi}$ cDC1s in response to LPS depend on intact TLR4 signaling in cDCs. However, the autocrine production of TNF-α is not essential for these specific outcomes, and instead, the TNF-α-mediated ablation is also extended in *trans* to those BTLA$^{hi}$ cDC1s that could not sense the original innate signal. A comprehensive ablation of the tolerogenic population is robustly propagated even if only a minor proportion of the BTLA$^{hi}$ cDC1s can respond to the initial innate stimulus. Further stressing the specific ablation of the BTLA$^{hi}$ cDC1s mediated by TNF-α, the expression of the death-inducing TNFR1 is highest in the BTLA$^{hi}$ cDC1s among all other cDCs. Therefore, by ablating the BTLA$^{hi}$ cDC1 population independently of the specific innate signals induced in the individual cDCs, functions of TNF-α and TNFR1 amplify the effects of the original innate signal to effectively extinguish the dominant capacity for the *de novo* conversion of antigen-specific pTreg cells during an acute immunogenic maturation process.

Similar to some other cytokines associated with maturation, the analogous “in trans” functions of TNF-α mediated by its different receptors can increase the activation and survival of some pro-immunogenic cDCs (Bachus et al., 2019; Bardou et al., 2021; Brunner et al., 2000; Le Bon et al., 2001; Maney et al., 2014; Sallusto and Lanzavecchia, 1994; Serbina et al., 2003; Sporri and Reis e Sousa, 2005; Sundquist and Wick, 2005; Trevejo et al., 2001; Winzler et al., 1997). Further, production of TNF-α by cDCs in the context of immune responses was proposed to depend on type I interferon and the relevant functions of its receptor IFNAR (Schaupp et al., 2020). Our findings now revealed that, in response to LPS, TNF-α is produced independently of IFNAR signaling and rapidly amplifies the ablation of tolerogenic BTLA$^{hi}$ cDC1s. Further underscoring these direct functions of TNF-α in mediating the ablation of BTLA$^{hi}$ cDC1s, a loss of BTLA$^{hi}$ cDC1s can be recapitulated by treatment with recombinant TNF-α *in vivo* in the absence of a specific exposure to innate signals.

Overall, by revealing a rapid death of BTLA$^{hi}$ cDC1s, our studies may also help to reconcile the results of the earlier observations of the LPS-induced death of cDCs and the most recent results that uncovered mechanisms to specifically prevent the inflammasome-mediated pyroptotic death of maturing cDCs with immunogenic functions (De Smedt et al., 1996; McDaniel et al., 2020; Qiu et al., 2009; Sundquist and Wick, 2009; Xu et al., 2017; Zhivaki et al., 2020). We propose that, whereas tolerogenic BTLA$^{hi}$ cDC1s are promptly and specifically ablated via the TNF-α-dependent mechanism, the remaining activated (mature) BTLA$^{lo}$ cDC1s and cDC2s are left to prime immune responses. Because cDC1s are well established to coordinate anti-viral and anti-tumor immune responses (Durai and Murphy, 2016; Eickhoff et al., 2015; Ferris et al., 2020), future studies will clarify the functions of BTLA$^{lo}$ cDC1s under such specific conditions *in vivo*.

The population of BTLA$^{lo}$ cDC1s that are preserved under pro-inflammatory conditions includes CCR7$^{+}$ cDC1s, possibly further consistent with the pre-existing specific pro-immunogenic programs in some CCR7$^{+}$ cDC1s (Ardouin et al., 2016). CCR7 governs

migration of cDCs (Ohl et al., 2004). Therefore, CCR7$^{hi}$ cDCs are considered to have migratory properties, and these cDCs play multiple roles in the initiation of effector responses under pro-inflammatory conditions as well as in the orchestration of tolerance, particularly that limiting anti-tumor responses (Bajana et al., 2012; GeurtsvanKessel et al., 2008; Ghiringhelli et al., 2005; Harimoto et al., 2013; Jenkins et al., 2021; Kim et al., 2010; Krishnaswamy et al., 2018; Maier et al., 2020; Scheinecker et al., 2002; Wang et al., 2019). Migratory cDCs transport antigens from parenchymal tissues to the lymph nodes in the steady state (Randolph et al., 2008) and, in the case of some respiratory infections, also to the spleen (Jenkins et al., 2021; Sichien et al., 2017). However, systemic soluble antigens are also delivered directly to cDCs present in the lymphoid organs, such as to spleen via the bloodstream (Bourque and Hawiger, 2022; Eisenbarth, 2019). Particularly, pTreg cells are readily induced in response to antigens that can be delivered either directly or indirectly to lymphoid organs (Iberg et al., 2017; Idoyaga et al., 2013; Jones et al., 2016). The *de novo* induction of such antigen-specific pTreg cells is compromised *in vivo* in the absence of specific tolerogenic functions of BTLA$^{hi}$ cDC1s (Iberg et al., 2017; Jones et al., 2016). We now found that BTLA$^{hi}$ cDC1s have a low expression of CCR7, and in the steady state, these BTLA$^{hi}$(CCR7$^{lo}$) cells constitute the major population of cDC1s within the spleen, and in the LNs, they correspond to previously characterized cells with “resident” characteristic (Crozat et al., 2011; Idoyaga et al., 2013). However, it may be difficult to unequivocally functionally distinguish migratory and resident systemic cDC populations *in vivo*. Most crucially, upon a specific pro-inflammatory activation, the BTLA$^{hi}$ cDCs die rapidly in order to limit the mechanisms of tolerance. Therefore, we propose that a high expression of BTLA and the preferential ablation of tolerogenic BTLA$^{hi}$ cDC1s transcend “migratory” versus resident identities of the systemic cDCs that in the steady state induce pTreg cells in the peripheral lymphoid organs.

After they complete the process of T cell priming, individual mature cDCs may undergo programmed death and be eventually replaced by precursors forming in the BM (Chen et al., 2006; Stranges et al., 2007; Winzler et al., 1997). In contrast, our findings uncovered an acute ablation of the entire population of tolerogenic BTLA$^{hi}$ cDC1s immediately after the initiation of an immunogenic maturation process. Such a rapid ablation of tolerogenic cDCs results in a loss of the *de novo* induction of antigen-specific pTreg cells, consistent with an abrogation of tolerogenic mechanisms during an acute immunogenic maturation (Cabeza-Cabrerizo et al., 2021; Dalod et al., 2014; Iberg and Hawiger, 2020; Iwasaki and Medzhitov, 2015; Mellman, 2013; Steinman et al., 2003a). However, the long-term absence of tolerogenic cDCs and their capacity for the *de novo* induction of dominant mechanisms of tolerance dependent on antigen-specific pTreg cells would pose a risk for insufficient immunoregulation. Therefore, our results help to clarify the biological benefits of the rapid cDC turnover *in vivo* by revealing that the tolerogenic BTLA$^{hi}$ cDC1 population is promptly re-established within the lymphoid organs and remains sensitive to a subsequent pro-inflammatory stimulus. Overall, by revealing an ablation of tolerogenic cDCs and the role of TNF-α in this process, the current studies are directly relevant for the design of new vaccines and immunotherapies based on specific abrogation or enhancement of tolerogenic mechanisms as clinically desired.

### Limitations of the study

In our experiments, we have not explored the corresponding mechanisms in other tolerogenic cDCs, such as those present at the anatomical barriers, and instead focused on the systemic cDCs relevant for various autoimmune and immune responses. Our studies utilized LPS, an archetypical pro-inflammatory stimulus. The mechanisms involving other adjuvants, specific infections, and other pro-inflammatory states will require future studies.

## STAR★METHODS

### RESOURCE AVAILABILITY

**Lead contact—**Further information and requests for resources and reagents should be directed to and will be fulfilled by the lead contact, Daniel Hawiger (daniel.hawiger@health.slu.edu).

**Materials availability—**This study did not generate new, unique reagents.

### Data and code availability

- All data reported in this paper will be shared by the lead contact upon request.
- This paper does not report original code.
- Any additional information required to reanalyze the data reported in this work paper is available from the lead contact upon request.

### EXPERIMENTAL MODEL AND SUBJECT DETAILS

**Mice—**All mouse strains were available on a C57BL/6J background. *Btla*$^{-/-}$ (Sedy et al., 2005), *Casp3*$^{-/-}$ (Kuida et al., 1996), *Casp8*$^{fl/fl}$ (Beisner et al., 2005), *Cd19*-Cre (CD19-Cre) (Rickert et al., 1997), B6.MRL-Fas$^{lpr}$/J (*Fas*$^{lpr}$) (Watanabe-Fukunaga et al., 1992), *Foxp3*$^{RFP}$ (Wan and Flavell, 2005), *Ifnar1*$^{-/-}$ (Hayashi et al., 2002; MÜller et al., 1994; Prigge et al., 2015), *Itgax*-Cre (CD11c-Cre) (Caton et al., 2007), *Lyz2*-Cre (LysM-Cre) (Clausen et al., 1999), *Myd88*$^{fl/fl}$ (Hou et al., 2008), OTII TCR tg (Barnden et al., 1998), *Ripk3*$^{-/-}$ (JAX stock #025738), *Tlr4*$^{-/-}$ (Hayashi et al., 2002; McAlees et al., 2015), *Tlr4*$^{fl/fl}$ (McAlees et al., 2015), *Tnfrsf1a*$^{-/-}$ (Peschon et al., 1998), and *Ticam1*$^{-/-}$ (*Trif*$^{-/-}$) (Hoebe et al., 2003) mice were previously described and available from Jackson Laboratory. OTII TCR tg (Barnden et al., 1998) mice were crossed with *Foxp3*$^{RFP}$ (Wan and Flavell, 2005) reporter mice to derive OTII *Foxp3*$^{RFP}$ mice. *Ripk3*$^{-/-}$ (JAX stock #025738), *Casp3*$^{-/-}$ (Kuida et al., 1996), *Casp8*$^{fl/fl}$ (Beisner et al., 2005), and *Itgax*-Cre (CD11c-Cre) (Caton et al., 2007) mice were crossed to derive *Ripk3*$^{-/-}$*Casp3*$^{-/-}$*Casp8*$^{\Delta CD11c}$ mice. *Ticam1*$^{-/-}$ (*Trif*$^{-/-}$) (Hoebe et al., 2003) mice were crossed with *Myd88*$^{fl/fl}$ (Hou et al., 2008) and *Itgax*-Cre (CD11c-Cre) (Caton et al., 2007) mice to derive *Trif*$^{-/-}$*Myd88*$^{\Delta CD11c}$ mice. *Tlr4*$^{fl/fl}$ (McAlees et al., 2015) mice were crossed with *Itgax*-Cre (CD11c-Cre) (Caton et al., 2007), *Lyz2*-Cre (LysM-Cre) (Clausen et al., 1999), or *Cd19*-Cre (CD19-Cre) (Rickert et al., 1997) mice to derive *Tlr4*$^{\Delta CD11c}$, *Tlr4*$^{\Delta LysM}$, and *Tlr4*$^{\Delta CD19}$ mice, respectively. *Tlr4*$^{-/-}$ (Hayashi et al., 2002; McAlees et al., 2015) mice were crossed with *Tnfrsf1a*$^{-/-}$ (Peschon et al., 1998) mice to derive *Tlr4*$^{-/-}$*Tnfrsf1a*$^{-/-}$ mice. Some C57BL/6J WT mice were also bred onto congenic B6.SJL-Ptprc$^{a}$ Pepc$^{b}$/BoyJ (CD45.1) background. 6- to 9-week-old sex- (both male and

female) and age-matched mice were used for experiments. Mice were randomly assigned to experimental groups. All mice were maintained in our facility under specific pathogen free conditions and used in accordance with guidelines of the Saint Louis University Institutional Animal Care and Use Committee.

## METHOD DETAILS

**cDC preparation—**Unless otherwise noted, spleens and peripheral (axial, brachial, and inguinal) lymph nodes were isolated and analyzed separately. To isolate cDCs, spleens and lymph nodes were dissected, individually mechanically fragmented with forceps and 30-gauge needles (BD), and treated with 2.5mg/mL Collagenase D (Roche) in RPMI 1640 media (Hyclone) supplemented with 5% fetal bovine serum (FBS) (Gemini Bio), Penicillin/Streptomycin (100U/mL), HEPES (10mM), Sodium Pyruvate (1mM), and 2-Mercaptoethanol (55μM) (all Gibco) at 37°C for 37 minutes, followed by incubation with EDTA (10mM) for 5 min at 37°C. After incubation, cells were passed through 100μm strainers (VWR) and washed using Hanks' Balanced Salt Solution (Gibco) supplemented with 2% FBS and 1mM EDTA to obtain single cell suspensions.

**Flow cytometry—**For analysis of T cells, spleens and lymph nodes were dissected and passed through 70μm strainers (Fisherbrand) to obtain single cell suspensions. cDCs were processed as above. Following lysis of red blood cells (RBCs) with ammonium chloride solution (0.16M) for 5 minutes at room temperature, single cell suspensions were washed with Dulbecco's phosphate buffered saline (DPBS; referred to as "PBS" throughout the text) (Hyclone) supplemented with 5% FBS and stained with Zombie Aqua Live/Dead viability dye (BioLegend) for 15 minutes at room temperature. Cells were then stained with Fc block (anti-CD16/32, clone 2.4G2; purified in-house using Protein G Sepharose Beads (GE Healthcare) from supernatants of corresponding hybridomas (ATCC) that were concentrated with ammonium sulfate) for 15 minutes at room temperature. For surface staining, cells were then incubated with fluorochrome-conjugated antibodies diluted in PBS supplemented with 2% FBS for 30 minutes on ice. After incubation, cells were washed twice and strained through 35μm strainers into FACS tubes (BD) for acquisition. To conduct staining for surface expression of CCR7, cells were stained with anti-CCR7 fluorochrome-conjugated antibody (BioLegend) diluted in PBS supplemented with 2% FBS for 30 minutes at 37°C prior to incubation with other surface marker antibodies. All samples were acquired on LSRII or BDFortessa (BD) instruments. Data was analyzed using FlowJo 10 software (FlowJo, LLC).

**Intracellular cytokine staining—**To conduct intracellular staining for TNF-α, spleens were processed and stained for surface markers as described above. Cells were then fixed and permeabilized using Cytofix-Cytoperm buffers (BD) according to the manufacturer's protocol and stained for intracellular TNF-α using a fluorochrome-conjugated anti-TNF-α antibody (BioLegend) for 30 minutes at 4°C.

**Bone marrow chimeras—**Wild-type recipient mice were placed on Sulfamethoxazole/Trimethoprim (SulfaTrim) antibiotic water for approximately one week prior to irradiation. Mice were lethally irradiated (10 Gy) approximately 6 hours prior to bone marrow (BM)

transfer. Congenically-labeled donor BM was obtained from indicated groups of mice. Briefly, donor mice were sacrificed, and BM was flushed from the femurs and tibias with a 30-gauge needle using PBS supplemented with 5% FBS. After red blood cell lysis, cells were washed twice in PBS and counted. Cells from mice of the indicated genotypes were mixed together at the indicated ratios, and 10–12 million total cells were injected intravenously into the tail vein of each recipient mouse. Recipient mice were kept on SulfaTrim antibiotic water for about 2 weeks post-BM transfer. 5 weeks after BM transfer, chimerism was verified by flow cytometry of blood. Chimera mice were utilized for experiments at least 6 weeks after BM transfer.

***In vivo* TLR stimulation—**Ultrapure Lipopolysaccharide (LPS) from *Escherichia coli* 0111:B4 (InvivoGen) was diluted in PBS and injected intraperitoneally into each mouse at defined doses and at specific time points as indicated in corresponding figure legends.

***In vivo* TNF-α stimulation—**Carrier-free recombinant mouse TNF-α (Biolegend) was diluted in PBS and injected intraperitoneally into each mouse at 4.5 μg/mouse.

***In vivo* TNF-α blockade—**250 μg blocking anti-TNF-α antibody (clone XT3.11) or 250 μg rat IgG1 isotype control (anti-horseradish peroxidase; clone HRPN) (both BioXcell) was injected intraperitoneally into each mouse 3.5 hours prior to administration of LPS or PBS. For experiments analyzed 48 hours after LPS administration, mice were injected a second time with 250 μg anti-TNFα antibody or isotype control antibody 24 hours after LPS administration.

**FACS-based TUNEL assay—**The APO-BrdU TUNEL kit (BD) was used to detect DNA strand breaks. cDCs were prepared as described above prior to enrichment by negative magnetic streptavidin microbead selection (Miltenyi) to exclude T cells (CD3ε), B cells (B220), and NK cells (CD49b) (biotinylated antibodies from BioLegend). Cells were then stained for cell surface markers as described above prior to TUNEL analysis according to the manufacturer's protocol.

**T Cell adoptive transfers—**Spleens and peripheral lymph nodes of OT-II *Foxp3*$^{RFP}$ donor mice were pooled together and enriched by depletion. CD4$^{+}$ T cells were enriched by negative magnetic streptavidin microbead selection (Miltenyi), which excluded cells expressing the surface molecules CD8α, B220, CD11b, CD11c, and CD49b (biotinylated antibodies from BioLegend). Enriched Foxp3(RFP)$^{neg}$ CD25$^{neg}$ cells were sorted on FACSAria Fusion or FACSAriaIII (BD) instruments. After sorting, cells were washed twice in PBS and counted. 3–5 million cells were injected intravenously into the tail vein of each recipient mouse.

***In vivo* delivery of antigens to cDCs—**OT-II TCR tg T cells were activated *in vivo* by cognate OVA$_{323–339}$ antigen that was delivered by anti-DEC-OVA, a recombinant chimeric antibody specific for DEC-205 (Hawiger et al., 2010; Iberg and Hawiger, 2019). Chimeric antibodies were expressed in Expi293 cells (ThermoFisher) as previously described (Fang et al., 2017). Cellular supernatants were concentrated using a Vivaflow 50R cassette (Sartorius), and antibodies were purified using Protein G Sepharose Beads (GE Healthcare)

as described in (Jones et al., 2016). Chimeric antibodies were injected intraperitoneally at 125 ng/mouse in PBS as previously established (Jones et al., 2016).

**Genomic DNA analysis—**To check for germline deletion of *Tlr4* in *Tlr4*$^{\Delta CD11c}$ mice, genomic DNA was extracted from ear biopsies of mice and analyzed by PCR using the following primers: Tlr4-F: 5′-TGACCACCCATATTGCCTATAC-3′ and Tlr4-R: 5′-TGATGGTGTGAGCAGGAGAG-3′. Products were run on a 2% agarose gel and imaged.

### QUANTIFICATION AND STATISTICAL ANALYSES

Sex- and age-matched mice of specified genotypes were randomly assigned into individual experimental groups. Data are presented as mean ± standard error of the mean (SEM) or mean ± standard deviation (SD). Group sizes were determined based on the results of preliminary experiments. No statistical method was used to predetermine sample size. *p* values were calculated in Prism 9 (GraphPad Software) using unpaired two-tailed *t* tests, one-way ANOVAs with Tukey's multiple comparisons, or two-way ANOVAs with Šídák's multiple comparisons, as indicated in corresponding figure legends. Differences were considered to be statistically significant when p % 0.05.

## Supplementary Material

Refer to Web version on PubMed Central for supplementary material.

## ACKNOWLEDGMENTS

The authors would like to thank Joy Eslick and Sherri L. Koehm (Saint Louis University Flow Cytometry Core) for expert help with flow cytometry. This work was supported in part by grants from National Institute of Allergy and Infectious Diseases of the National Institutes of Health (R01AI113903) and National Multiple Sclerosis Society (RG-1902-33632), both to D.H. The graphical abstract was created using Biorender.com.

## REFERENCES

Abram CL, Roberge GL, Hu Y, and Lowell CA (2014). Comparative analysis of the efficiency and specificity of myeloid-Cre deleting strains using ROSA-EYFP reporter mice. J. Immunol. Methods 408, 89–100. [PubMed: 24857755]

Albert ML, Pearce SF, Francisco LM, Sauter B, Roy P, Silverstein RL, and Bhardwaj N (1998). Immature dendritic cells phagocytose apoptotic cells via alphavbeta5 and CD36, and cross-present antigens to cytotoxic T lymphocytes. J. Exp. Med 188, 1359–1368. [PubMed: 9763615]

Anderson AE, Swan DJ, Sayers BL, Harry RA, Patterson AM, von Delwig A, Robinson JH, Isaacs JD, and Hilkens CM (2009). LPS activation is required for migratory activity and antigen presentation by tolerogenic dendritic cells. J. Leukoc. Biol 85, 243–250. [PubMed: 18971286]

Ardouin L, Luche H, Chelbi R, Carpentier S, Shawket A, Montanana Sanchis F, Santa Maria C, Grenot P, Alexandre Y, Gregoire C, et al. (2016). Broad and largely concordant molecular changes characterize tolerogenic and immunogenic dendritic cell maturation in thymus and periphery. Immunity 45, 305–318. [PubMed: 27533013]

Arpaia N, Campbell C, Fan X, Dikiy S, van der Veeken J, Deroos P, Liu H, Cross JR, Pfeffer K, Coffer PJ, et al. (2013). Metabolites produced by commensal bacteria promote peripheral regulatory T-cell generation. Nature 504, 451–455. [PubMed: 24226773]

Bachus H, Kaur K, Papillion AM, Marquez-Lago TT, Yu Z, Ballesteros-Tato A, Matalon S, and Leon B (2019). Impaired tumor-necrosis-factor-alpha-driven dendritic cell activation limits lipopolysaccharide-induced protection from allergic inflammation in infants. Immunity 50, 225–240.e24. [PubMed: 30635238]

Bajana S, Roach K, Turner S, Paul J, and Kovats S (2012). IRF4 promotes cutaneous dendritic cell migration to lymph nodes during homeostasis and inflammation. J. Immunol 189, 3368–3377. [PubMed: 22933627]

Baratin M, Foray C, Demaria O, Habbeddine M, Pollet E, Maurizio J, Verthuy C, Davanture S, Azukizawa H, Flores-Langarica A, et al. (2015). Homeostatic NF-kappaB signaling in steady-state migratory dendritic cells regulates immune homeostasis and tolerance. Immunity 42, 627–639. [PubMed: 25862089]

Bardou M, Postat J, Loaec C, Lemaitre F, Ronteix G, Garcia Z, and Bousso P (2021). Quorum sensing governs collective dendritic cell activation *in vivo*. EMBO J 40, e107176. [PubMed: 34124789]

Barnden MJ, Allison J, Heath WR, and Carbone FR (1998). Defective TCR expression in transgenic mice constructed using cDNA-based alpha- and beta-chain genes under the control of heterologous regulatory elements. Immunol. Cell Biol 76, 34–40. [PubMed: 9553774]

Beisner DR, Ch'en IL, Kolla RV, Hoffmann A, and Hedrick SM (2005). Cutting edge: innate immunity conferred by B cells is regulated by caspase-8. J. Immunol 175, 3469–3473. [PubMed: 16148088]

Belz GT, Behrens GM, Smith CM, Miller JF, Jones C, Lejon K, Fathman CG, Mueller SN, Shortman K, Carbone FR, et al. (2002). The CD8alpha(+) dendritic cell is responsible for inducing peripheral self-tolerance to tissue-associated antigens. J. Exp. Med 196, 1099–1104. [PubMed: 12391021]

Bourque J, and Hawiger D (2018). Immunomodulatory bonds of the partnership between dendritic cells and T cells. Crit. Rev. Immunol 38, 379–401. [PubMed: 30792568]

Bourque J, and Hawiger D (2019). The BTLA–HVEM–CD5 immunoregulatory Axis–an instructive mechanism governing pTreg cell differentiation. Front. Immunol 10, 1163. [PubMed: 31191536]

Bourque J, and Hawiger D (2022). Variegated outcomes of T cell activation by dendritic cells in the steady state. J. Immunol 208, 539–547. [PubMed: 35042789]

Brunner C, Seiderer J, Schlamp A, Bidlingmaier M, Eigler A, Haimerl W, Lehr HA, Krieg AM, Hartmann G, and Endres S (2000). Enhanced dendritic cell maturation by TNF-alpha or cytidine-phosphate-guanosine DNA drives T cell activation in vitro and therapeutic anti-tumor immune responses *in vivo*. J. Immunol 165, 6278–6286. [PubMed: 11086063]

Cabeza-Cabrerizo M, Cardoso A, Minutti CM, Pereira da Costa M, and Reis ESC (2021). Dendritic cells revisited. Annu. Rev. Immunol 39, 131–166. [PubMed: 33481643]

Caton ML, Smith-Raska MR, and Reizis B (2007). Notch-RBP-J signaling controls the homeostasis of CD8- dendritic cells in the spleen. J. Exp. Med 204, 1653–1664. [PubMed: 17591855]

Chen M, Wang YH, Wang Y, Huang L, Sandoval H, Liu YJ, and Wang J (2006). Dendritic cell apoptosis in the maintenance of immune tolerance. Science 311, 1160–1164. [PubMed: 16497935]

Clausen BE, Burkhardt C, Reith W, Renkawitz R, and Forster I (1999). Conditional gene targeting in macrophages and granulocytes using LysMcre mice. Transgenic Res. 8, 265–277. [PubMed: 10621974]

Crozat K, Tamoutounour S, Vu Manh TP, Fossum E, Luche H, Ardouin L, Guilliams M, Azukizawa H, Bogen B, Malissen B, et al. (2011). Cutting edge: expression of XCR1 defines mouse lymphoid-tissue resident and migratory dendritic cells of the CD8alpha+ type. J. Immunol 187, 4411–4415. [PubMed: 21948982]

Cummings RJ, Barbet G, Bongers G, Hartmann BM, Gettler K, Muniz L, Furtado GC, Cho J, Lira SA, and Blander JM (2016). Different tissue phagocytes sample apoptotic cells to direct distinct homeostasis programs. Nature 539, 565–569. [PubMed: 27828940]

Dalod M, Chelbi R, Malissen B, and Lawrence T (2014). Dendritic cell maturation: functional specialization through signaling specificity and transcriptional programming. EMBO J. 33, 1104–1116. [PubMed: 24737868]

De Smedt T, Pajak B, Muraille E, Lespagnard L, Heinen E, De Baetselier P, Urbain J, Leo O, and Moser M (1996). Regulation of dendritic cell numbers and maturation by lipopolysaccharide *in vivo*. J. Exp. Med 184, 1413–1424. [PubMed: 8879213]

De Trez C, Pajak B, Brait M, Glaichenhaus N, Urbain J, Moser M, Lauvau G, and Muraille E (2005). TLR4 and Toll-IL-1 receptor domain-containing adapter-inducing IFN-beta, but not MyD88, regulate Escherichia coliinduced dendritic cell maturation and apoptosis *in vivo*. J. Immunol 175, 839–846. [PubMed: 16002681]

Durai V, and Murphy KM (2016). Functions of murine dendritic cells. Immunity 45, 719–736. [PubMed: 27760337]

Edwards AD, Diebold SS, Slack EM, Tomizawa H, Hemmi H, Kaisho T, Akira S, and Reis e Sousa C (2003). Toll-like receptor expression in murine DC subsets: lack of TLR7 expression by CD8 alpha+ DC correlates with unresponsiveness to imidazoquinolines. Eur. J. Immunol 33, 827–833. [PubMed: 12672047]

Eickhoff S, Brewitz A, Gerner MY, Klauschen F, Komander K, Hemmi H, Garbi N, Kaisho T, Germain RN, and Kastenmuller W (2015). Robust anti-viral immunity requires multiple distinct T cell-dendritic cell interactions. Cell 162, 1322–1337. [PubMed: 26296422]

Eisenbarth SC (2019). Dendritic cell subsets in T cell programming: location dictates function. Nat. Rev. Immunol 19, 89–103. [PubMed: 30464294]

Esterhazy D, Canesso MCC, Mesin L, Muller PA, de Castro TBR, Lockhart A, ElJalby M, Faria AMC, and Mucida D (2019). Compartmentalized gut lymph node drainage dictates adaptive immune responses. Nature 569, 126–130. [PubMed: 30988509]

Falvo JV, Tsytsykova AV, and Goldfeld AE (2010). Transcriptional control of the TNF gene. Curr. Dir. Autoimmun 11, 27–60. [PubMed: 20173386]

Fang XT, Sehlin D, Lannfelt L, Syvänen S, and Hultqvist G (2017). Efficient and inexpensive transient expression of multispecific multivalent antibodies in Expi293 cells. Biol. Proced. Online 19, 11. [PubMed: 28932173]

Ferris ST, Durai V, Wu R, Theisen DJ, Ward JP, Bern MD, Davidson J.T.t., Bagadia P, Liu T, Briseno CG, et al. (2020). cDC1 prime and are licensed by CD4(+) T cells to induce anti-tumour immunity. Nature 584, 624–629. [PubMed: 32788723]

Fitzgerald KA, and Kagan JC (2020). Toll-like receptors and the control of immunity. Cell 180, 1044–1066. [PubMed: 32164908]

Fonseca DM, Hand TW, Han SJ, Gerner MY, Glatman Zaretsky A, Byrd AL, Harrison OJ, Ortiz AM, Quinones M, Trinchieri G, et al. (2015). Microbiota-dependent sequelae of acute infection compromise tissue-specific immunity. Cell 163, 354–366. [PubMed: 26451485]

Fuertes Marraco SA, Scott CL, Bouillet P, Ives A, Masina S, Vremec D, Jansen ES, O'Reilly LA, Schneider P, Fasel N, et al. (2011). Type I interferon drives dendritic cell apoptosis via multiple BH3-only proteins following activation by PolyIC *in vivo*. PLoS One 6, e20189. [PubMed: 21674051]

GeurtsvanKessel CH, Willart MAM, van Rijt LS, Muskens F, Kool M, Baas C, Thielemans K, Bennett C, Clausen B.r.E., Hoogsteden HC, et al. (2008). Clearance of influenza virus from the lung depends on migratory langerin+CD11b but not plasmacytoid dendritic cells. J. Exp. Med 205, 1621–1634. [PubMed: 18591406]

Ghiringhelli F, Puig PE, Roux S, Parcellier A, Schmitt E, Solary E, Kroemer G, Martin F, Chauffert B, and Zitvogel L (2005). Tumor cells convert immature myeloid dendritic cells into TGF-beta-secreting cells inducing CD4+CD25+ regulatory T cell proliferation. J. Exp. Med 202, 919–929. [PubMed: 16186184]

Guilliams M, Crozat K, Henri S, Tamoutounour S, Grenot P, Devilard E, de Bovis B, Alexopoulou L, Dalod M, and Malissen B (2010). Skin-draining lymph nodes contain dermis-derived CD103(−) dendritic cells that constitutively produce retinoic acid and induce Foxp3(+) regulatory T cells. Blood 115, 1958–1968. [PubMed: 20068222]

Guilliams M, Dutertre CA, Scott CL, McGovern N, Sichien D, Chakarov S, Van Gassen S, Chen J, Poidinger M, De Prijck S, et al. (2016). Unsupervised high-dimensional analysis aligns dendritic cells across tissues and species. Immunity 45, 669–684. [PubMed: 27637149]

Guilliams M, Ginhoux F, Jakubzick C, Naik SH, Onai N, Schraml BU, Segura E, Tussiwand R, and Yona S (2014). Dendritic cells, monocytes and macrophages: a unified nomenclature based on ontogeny. Nat. Rev. Immunol 14, 571–578. [PubMed: 25033907]

Hammer GE, and Ma A (2013). Molecular control of steady-state dendritic cell maturation and immune homeostasis. Annu. Rev. Immunol 31, 743–791. [PubMed: 23330953]

Harimoto H, Shimizu M, Nakagawa Y, Nakatsuka K, Wakabayashi A, Sakamoto C, and Takahashi H (2013). Inactivation of tumor-specific CD8(+) CTLs by tumor-infiltrating tolerogenic dendritic cells. Immunol. Cell Biol 91, 545–555. [PubMed: 24018532]

Hawiger D, Wan YY, Eynon EE, and Flavell RA (2010). The transcription cofactor Hopx is required for regulatory T cell function in dendritic cell-mediated peripheral T cell unresponsiveness. Nat. Immunol 11, 962–968. [PubMed: 20802482]

Hayashi S, Lewis P, Pevny L, and McMahon AP (2002). Efficient gene modulation in mouse epiblast using a Sox2Cre transgenic mouse strain. Mech. Dev 119, S97–S101. [PubMed: 14516668]

Helft J, Bottcher J, Chakravarty P, Zelenay S, Huotari J, Schraml BU, Goubau D, and Reis e Sousa C (2015). GM-CSF mouse bone marrow cultures comprise a heterogeneous population of CD11c(+)MHCII(+) macrophages and dendritic cells. Immunity 42, 1197–1211. [PubMed: 26084029]

Henderson JG, Opejin A, Jones A, Gross C, and Hawiger D (2015). CD5 instructs extrathymic regulatory T cell development in response to self and tolerizing antigens. Immunity 42, 471–483. [PubMed: 25786177]

Hildner K, Edelson BT, Purtha WE, Diamond M, Matsushita H, Kohyama M, Calderon B, Schraml BU, Unanue ER, Diamond MS, et al. (2008). Batf3 deficiency reveals a critical role for CD8alpha+ dendritic cells in cytotoxic T cell immunity. Science 322, 1097–1100. [PubMed: 19008445]

Hoebe K, Du X, Georgel P, Janssen E, Tabeta K, Kim SO, Goode J, Lin P, Mann N, Mudd S, et al. (2003). Identification of Lps2 as a key transducer of MyD88-independent TIR signalling. Nature 424, 743–748. [PubMed: 12872135]

Hou B, Reizis B, and DeFranco AL (2008). Toll-like receptors activate innate and adaptive immunity by using dendritic cell-intrinsic and -extrinsic mechanisms. Immunity 29, 272–282. [PubMed: 18656388]

Iberg CA, and Hawiger D (2019). Advancing immunomodulation by *in vivo* antigen delivery to DEC-205 and other cell surface molecules using recombinant chimeric antibodies. Int. Immunopharmacol 73, 575–580. [PubMed: 31228685]

Iberg CA, and Hawiger D (2020). Natural and induced tolerogenic dendritic cells. J. Immunol 204, 733–744. [PubMed: 32015076]

Iberg CA, Jones A, and Hawiger D (2017). Dendritic cells as inducers of peripheral tolerance. Trends Immunol 38, 793–804. [PubMed: 28826942]

Idoyaga J, Fiorese C, Zbytnuik L, Lubkin A, Miller J, Malissen B, Mucida D, Merad M, and Steinman RM (2013). Specialized role of migratory dendritic cells in peripheral tolerance induction. J. Clin. Invest 123, 844–854. [PubMed: 23298832]

Iwasaki A, and Medzhitov R (2015). Control of adaptive immunity by the innate immune system. Nat. Immunol 16, 343–353. [PubMed: 25789684]

Iyoda T, Shimoyama S, Liu K, Omatsu Y, Akiyama Y, Maeda Y, Takahara K, Steinman RM, and Inaba K (2002). The CD8+ dendritic cell subset selectively endocytoses dying cells in culture and *in vivo*. J. Exp. Med 195, 1289–1302. [PubMed: 12021309]

Jenkins MM, Bachus H, Botta D, Schultz MD, Rosenberg AF, Leon B, and Ballesteros-Tato A (2021). Lung dendritic cells migrate to the spleen to prime long-lived TCF1(hi) memory CD8(+) T cell precursors after influenza infection. Sci. Immunol 6, eabg6895. [PubMed: 34516781]

Jiang A, Bloom O, Ono S, Cui W, Unternaehrer J, Jiang S, Whitney JA, Connolly J, Banchereau J, and Mellman I (2007). Disruption of E-cadherin-mediated adhesion induces a functionally distinct pathway of dendritic cell maturation. Immunity 27, 610–624. [PubMed: 17936032]

Jones A, Bourque J, Kuehm L, Opejin A, Teague RM, Gross C, and Hawiger D (2016). Immunomodulatory functions of BTLA and HVEM govern induction of extrathymic regulatory T cells and tolerance by dendritic cells. Immunity 45, 1066–1077. [PubMed: 27793593]

Jones A, and Hawiger D (2017). Peripherally induced regulatory T cells: recruited protectors of the central nervous system against autoimmune neuroinflammation. Front. Immunol 8, 532. [PubMed: 28536579]

Jones A, Opejin A, Henderson JG, Gross C, Jain R, Epstein JA, Flavell RA, and Hawiger D (2015). Peripherally induced tolerance depends on peripheral regulatory T cells that require hopx to inhibit intrinsic IL-2 expression. J. Immunol 195, 1489–1497. [PubMed: 26170384]

Kaisho T, Takeuchi O, Kawai T, Hoshino K, and Akira S (2001). Endotoxin-induced maturation of MyD88-deficient dendritic cells. J. Immunol 166, 5688–5694. [PubMed: 11313410]

Kamath AT, Pooley J, O'Keeffe MA, Vremec D, Zhan Y, Lew AM, D'Amico A, Wu L, Tough DF, and Shortman K (2000). The development, maturation, and turnover rate of mouse spleen dendritic cell populations. J. Immunol 165, 6762–6770. [PubMed: 11120796]

Kashem SW, Haniffa M, and Kaplan DH (2017). Antigen-Presenting cells in the skin. Annu. Rev. Immunol 35, 469–499. [PubMed: 28226228]

Kim TS, Hufford MM, Sun J, Fu Y-X, and Braciale TJ (2010). Antigen persistence and the control of local T cell memory by migrant respiratory dendritic cells after acute virus infection. J. Exp. Med 207, 1161–1172. [PubMed: 20513748]

Kobayashi Y, Iwata A, Suzuki K, Suto A, Kawashima S, Saito Y, Owada T, Kobayashi M, Watanabe N, and Nakajima H (2013). B and T lymphocyte attenuator inhibits LPS-induced endotoxic shock by suppressing Toll-like receptor 4 signaling in innate immune cells. Proc. Natl. Acad. Sci. U S A 110, 5121–5126. [PubMed: 23479601]

Kolb JP, Oguin TH 3rd, Oberst A, and Martinez J (2017). Programmed cell death and inflammation: winter is coming. Trends Immunol. 38, 705–718. [PubMed: 28734635]

Krishnaswamy JK, Alsen S, Yrlid U, Eisenbarth SC, and Williams A (2018). Determination of T Follicular helper cell fate by dendritic cells. Front. Immunol 9, 2169. [PubMed: 30319629]

Kuida K, Zheng TS, Na S, Kuan C, Yang D, Karasuyama H, Rakic P, and Flavell RA (1996). Decreased apoptosis in the brain and premature lethality in CPP32-deficient mice. Nature 384, 368–372. [PubMed: 8934524]

Le Bon A, Schiavoni G, D'Agostino G, Gresser I, Belardelli F, and Tough DF (2001). Type i interferons potently enhance humoral immunity and can promote isotype switching by stimulating dendritic cells *in vivo*. Immunity 14, 461–470. [PubMed: 11336691]

Li CC, Munitic I, Mittelstadt PR, Castro E, and Ashwell JD (2015). Suppression of dendritic cell-derived IL-12 by endogenous glucocorticoids is protective in LPS-induced sepsis. PLOS Biol. 13, e1002269. [PubMed: 26440998]

Liu K, Waskow C, Liu X, Yao K, Hoh J, and Nussenzweig M (2007). Origin of dendritic cells in peripheral lymphoid organs of mice. Nat. Immunol 8, 578–583. [PubMed: 17450143]

Maier B, Leader AM, Chen ST, Tung N, Chang C, LeBerichel J, Chudnovskiy A, Maskey S, Walker L, Finnigan JP, et al. (2020). A conserved dendritic-cell regulatory program limits antitumour immunity. Nature 580, 257–262. [PubMed: 32269339]

Maney NJ, Reynolds G, Krippner-Heidenreich A, and Hilkens CMU (2014). Dendritic cell maturation and survival are differentially regulated by TNFR1 and TNFR2. J. Immunol 193, 4914–4923. [PubMed: 25288570]

Manh TP, Alexandre Y, Baranek T, Crozat K, and Dalod M (2013). Plasmacytoid, conventional, and monocyte-derived dendritic cells undergo a profound and convergent genetic reprogramming during their maturation. Eur. J. Immunol 43, 1706–1715. [PubMed: 23553052]

Manicassamy S, and Pulendran B (2011). Dendritic cell control of tolerogenic responses. Immunol. Rev 241, 206–227. [PubMed: 21488899]

Mattei F, Bracci L, Tough DF, Belardelli F, and Schiavoni G (2009). Type I IFN regulate DC turnover *in vivo*. Eur. J. Immunol 39, 1807–1818. [PubMed: 19544312]

McAlees JW, Whitehead GS, Harley IT, Cappelletti M, Rewerts CL, Holdcroft AM, Divanovic S, Wills-Karp M, Finkelman FD, Karp CL, et al. (2015). Distinct Tlr4-expressing cell compartments control neutrophilic and eosinophilic airway inflammation. Mucosal Immunol 8, 863–873. [PubMed: 25465099]

McDaniel MM, Kottyan LC, Singh H, and Pasare C (2020). Suppression of inflammasome activation by IRF8 and IRF4 in cDCs is critical for T cell priming. Cell Rep. 31, 107604. [PubMed: 32375053]

Melillo JA, Song L, Bhagat G, Blazquez AB, Plumlee CR, Lee C, Berin C, Reizis B, and Schindler C (2010). Dendritic cell (DC)-Specific targeting reveals Stat3 as a negative regulator of DC function. J. Immunol 184, 2638. [PubMed: 20124100]

Mellman I (2013). Dendritic cells: master regulators of the immune response. Cancer Immunol. Res 1, 145–149. [PubMed: 24777676]

Menges M, Rossner S, Voigtlander C, Schindler H, Kukutsch NA, Bogdan C, Erb K, Schuler G, and Lutz MB (2002). Repetitive injections of dendritic cells matured with tumor necrosis factor alpha

induce antigen-specific protection of mice from autoimmunity. J. Exp. Med 195, 15–21. [PubMed: 11781361]

Miller JC, Brown BD, Shay T, Gautier EL, Jojic V, Cohain A, Pandey G, Leboeuf M, Elpek KG, Helft J, et al. (2012). Deciphering the transcriptional network of the dendritic cell lineage. Nat. Immunol 13, 888–899. [PubMed: 22797772]

Müller U, Steinhoff U, Reis LF, Hemmi S, Pavlovic J, Zinkernagel RM, and Aguet M (1994). Functional role of type I and type II interferons in antiviral defense. Science 264, 1918–1921. [PubMed: 8009221]

Murphy TL, and Murphy KM (2010). Slow down and survive: enigmatic immunoregulation by BTLA and HVEM. Annu. Rev. Immunol 28, 389–411. [PubMed: 20307212]

Nagata S, and Tanaka M (2017). Programmed cell death and the immune system. Nat. Rev. Immunol 17, 333–340. [PubMed: 28163302]

Newton K, Sun X, and Dixit VM (2004). Kinase RIP3 is dispensable for normal NF-kappa Bs, signaling by the B-cell and T-cell receptors, tumor necrosis factor receptor 1, and Toll-like receptors 2 and 4. Mol. Cell Biol 24, 1464–1469. [PubMed: 14749364]

Ohl L, Mohaupt M, Czeloth N, Hintzen G, Kiafard Z, Zwirner J, Blankenstein T, Henning G, and Forster R (2004). CCR7 governs skin dendritic cell migration under inflammatory and steady-state conditions. Immunity 21, 279–288. [PubMed: 15308107]

Opejin A, Surnov A, Misulovin Z, Pherson M, Gross C, Iberg CA, Fallahee I, Bourque J, Dorsett D, and Hawiger D (2020). A two-step process of effector programming governs CD4(+) T cell fate determination induced by antigenic activation in the steady state. Cell Rep 33, 108424. [PubMed: 33238127]

Peschon JJ, Torrance DS, Stocking KL, Glaccum MB, Otten C, Willis CR, Charrier K, Morrissey PJ, Ware CB, and Mohler KM (1998). TNF receptor-deficient mice reveal divergent roles for p55 and p75 in several models of inflammation. J. Immunol 160, 943–952. [PubMed: 9551933]

Prigge JR, Hoyt TR, Dobrinen E, Capecchi MR, Schmidt EE, and Meissner N (2015). Type I IFNs act upon hematopoietic progenitors to protect and maintain hematopoiesis during Pneumocystis lung infection in mice. J. Immunol 195, 5347. [PubMed: 26519535]

Qiu CH, Miyake Y, Kaise H, Kitamura H, Ohara O, and Tanaka M (2009). Novel subset of CD8{alpha}+ dendritic cells localized in the marginal zone is responsible for tolerance to cell-associated antigens. J. Immunol 182, 4127–4136. [PubMed: 19299710]

Randolph GJ, Ochando J, and Partida-Sanchez S (2008). Migration of dendritic cell subsets and their precursors. Annu. Rev. Immunol 26, 293–316. [PubMed: 18045026]

Rickert RC, Roes J, and Rajewsky K (1997). B lymphocyte-specific, Cre-mediated mutagenesis in mice. Nucleic Acids Res. 25, 1317–1318. [PubMed: 9092650]

Russler-Germain EV, Yi J, Young S, Nutsch K, Wong HS, Ai TL, Chai JN, Durai V, Kaplan DH, Germain RN, et al. (2021). Gut Helicobacter presentation by multiple dendritic cell subsets enables context-specific regulatory T cell generation. Elife 10, e54792. [PubMed: 33533717]

Sallusto F, and Lanzavecchia A (1994). Efficient presentation of soluble antigen by cultured human dendritic cells is maintained by granulocyte/macrophage colony-stimulating factor plus interleukin 4 and downregulated by tumor necrosis factor alpha. J. Exp. Med 179, 1109–1118. [PubMed: 8145033]

Schaupp L, Muth S, Rogell L, Kofoed-Branzk M, Melchior F, Lienenklaus S, Ganal-Vonarburg SC, Klein M, Guendel F, Hain T, et al. (2020). Microbiota-induced type I interferons instruct a poised basal state of dendritic cells. Cell 181, 1080–1096.e19. [PubMed: 32380006]

Scheinecker C, McHugh R, Shevach EM, and Germain RN (2002). Constitutive presentation of a natural tissue autoantigen exclusively by dendritic cells in the draining lymph node. J. Exp. Med 196, 1079–1090. [PubMed: 12391019]

Sedy JR, Gavrieli M, Potter KG, Hurchla MA, Lindsley RC, Hildner K, Scheu S, Pfeffer K, Ware CF, Murphy TL, et al. (2005). B and T lymphocyte attenuator regulates T cell activation through interaction with herpesvirus entry mediator. Nat. Immunol 6, 90–98. [PubMed: 15568026]

Serbina NV, Salazar-Mather TP, Biron CA, Kuziel WA, and Pamer EG (2003). TNF/iNOS-producing dendritic cells mediate innate immune defense against bacterial infection. Immunity 19, 59–70. [PubMed: 12871639]

Shui JW, Steinberg MW, and Kronenberg M (2011). Regulation of inflammation, autoimmunity, and infection immunity by HVEM-BTLA signaling. J. Leukoc. Biol 89, 517–523. [PubMed: 21106644]

Sichien D, Lambrecht BN, Guilliams M, and Scott CL (2017). Development of conventional dendritic cells: from common bone marrow progenitors to multiple subsets in peripheral tissues. Mucosal Immunol 10, 831–844. [PubMed: 28198365]

Sporri R, and Reis e Sousa C (2005). Inflammatory mediators are insufficient for full dendritic cell activation and promote expansion of CD4+ T cell populations lacking helper function. Nat. Immunol 6, 163–170. [PubMed: 15654341]

Steinman RM (2012). Decisions about dendritic cells: past, present, and future. Annu. Rev. Immunol 30, 1–22. [PubMed: 22136168]

Steinman RM, Hawiger D, Liu K, Bonifaz L, Bonnyay D, Mahnke K, Iyoda T, Ravetch J, Dhodapkar M, Inaba K, et al. (2003a). Dendritic cell function *in vivo* during the steady state: a role in peripheral tolerance. Ann. N. Y. Acad. Sci 987, 15–25. [PubMed: 12727620]

Steinman RM, Hawiger D, and Nussenzweig MC (2003b). Tolerogenic dendritic cells. Annu. Rev. Immunol 21, 685–711. [PubMed: 12615891]

Stranges PB, Watson J, Cooper CJ, Choisy-Rossi CM, Stonebraker AC, Beighton RA, Hartig H, Sundberg JP, Servick S, Kaufmann G, et al. (2007). Elimination of antigen-presenting cells and autoreactive T cells by Fas contributes to prevention of autoimmunity. Immunity 26, 629–641. [PubMed: 17509906]

Sundquist M, and Wick MJ (2005). TNF-alpha-dependent and -independent maturation of dendritic cells and recruited CD11c(int)CD11b+ Cells during oral Salmonella infection. J. Immunol 175, 3287–3298. [PubMed: 16116221]

Sundquist M, and Wick MJ (2009). Salmonella induces death of CD8alpha(+) dendritic cells but not CD11c(int)CD11b(+) inflammatory cells *in vivo* via MyD88 and TNFR1. J. Leukoc. Biol 85, 225–234. [PubMed: 19004989]

Trevejo JM, Marino MW, Philpott N, Josien R, Richards EC, Elkon KB, and Falck-Pedersen E (2001). TNF-alpha -dependent maturation of local dendritic cells is critical for activating the adaptive immune response to virus infection. Proc. Natl. Acad. Sci. U S A 98, 12162–12167. [PubMed: 11593031]

Tussiwand R, Lee WL, Murphy TL, Mashayekhi M, Kc W, Albring JC, Satpathy AT, Rotondo JA, Edelson BT, Kretzer NM, et al. (2012). Compensatory dendritic cell development mediated by BATF-IRF interactions. Nature 490, 502–507. [PubMed: 22992524]

Vander Lugt B, Riddell J, Khan AA, Hackney JA, Lesch J, DeVoss J, Weirauch MT, Singh H, and Mellman I (2017). Transcriptional determinants of tolerogenic and immunogenic states during dendritic cell maturation. J. Cell Biol 216, 779–792. [PubMed: 28130292]

Vitali C, Mingozzi F, Broggi A, Barresi S, Zolezzi F, Bayry J, Raimondi G, Zanoni I, and Granucci F (2012). Migratory, and not lymphoid-resident, dendritic cells maintain peripheral self-tolerance and prevent autoimmunity via induction of iTreg cells. Blood 120, 1237–1245. [PubMed: 22760781]

Wajant H, and Siegmund D (2019). TNFR1 and TNFR2 in the control of the life and death balance of macrophages. Front. Cell Dev. Biol 7, 91. [PubMed: 31192209]

Wan YY, and Flavell RA (2005). Identifying Foxp3-expressing suppressor T cells with a bicistronic reporter. Proc. Natl. Acad. Sci. U S A 102, 5126–5131. [PubMed: 15795373]

Wang Y, Du X, Wei J, Long L, Tan H, Guy C, Dhungana Y, Qian C, Neale G, Fu YX, et al. (2019). LKB1 orchestrates dendritic cell metabolic quiescence and anti-tumor immunity. Cell Res. 29, 391–405. [PubMed: 30911060]

Watanabe-Fukunaga R, Brannan CI, Copeland NG, Jenkins NA, and Nagata S (1992). Lymphoproliferation disorder in mice explained by defects in Fas antigen that mediates apoptosis. Nature 356, 314–317. [PubMed: 1372394]

Winzler C, Rovere P, Rescigno M, Granucci F, Penna G, Adorini L, Zimmermann VS, Davoust J, and Ricciardi-Castagnoli P (1997). Maturation stages of mouse dendritic cells in growth factor-dependent long-term cultures. J. Exp. Med 185, 317–328. [PubMed: 9016880]

Xu L, Kwak M, Zhang W, Lee PC, and Jin JO (2017). Time-dependent effect of E. coli LPS in spleen DC activation *in vivo*: alteration of numbers, expression of co-stimulatory molecules, production of pro-inflammatory cytokines, and presentation of antigens. Mol. Immunol 85, 205–213. [PubMed: 28285188]

Yin X, Chen S, and Eisenbarth SC (2021). Dendritic cell regulation of T helper cells. Annu. Rev. Immunol 39, 759–790. [PubMed: 33710920]

Zanoni I, Ostuni R, Capuano G, Collini M, Caccia M, Ronchi AE, Rocchetti M, Mingozzi F, Foti M, Chirico G, et al. (2009). CD14 regulates the dendritic cell life cycle after LPS exposure through NFAT activation. Nature 460, 264–268. [PubMed: 19525933]

Zanoni I, Tan Y, Di Gioia M, Broggi A, Ruan J, Shi J, Donado CA, Shao F, Wu H, Springstead JR, et al. (2016). An endogenous caspase-11 ligand elicits interleukin-1 release from living dendritic cells. Science 352, 1232–1236. [PubMed: 27103670]

Zhivaki D, Borriello F, Chow OA, Doran B, Fleming I, Theisen DJ, Pallis P, Shalek AK, Sokol CL, Zanoni I, et al. (2020). Inflammasomes within hyperactive murine dendritic cells stimulate long-lived T cell-mediated anti-tumor immunity. Cell Rep. 33, 108381. [PubMed: 33207188]

Zhou F, Ciric B, Zhang GX, and Rostami A (2014). Immunotherapy using lipopolysaccharide-stimulated bone marrow-derived dendritic cells to treat experimental autoimmune encephalomyelitis. Clin. Exp. Immunol 178, 447–458. [PubMed: 25138204]

## Highlights

- LPS induces TNF-α, which ablates tolerogenic BTLA$^{hi}$ cDCs *in vivo*
- TNFR1-dependent death of tolerogenic cDCs amplifies the innate stimulus
- Transient remodeling of the cDC functional landscape prevents tolerogenic responses

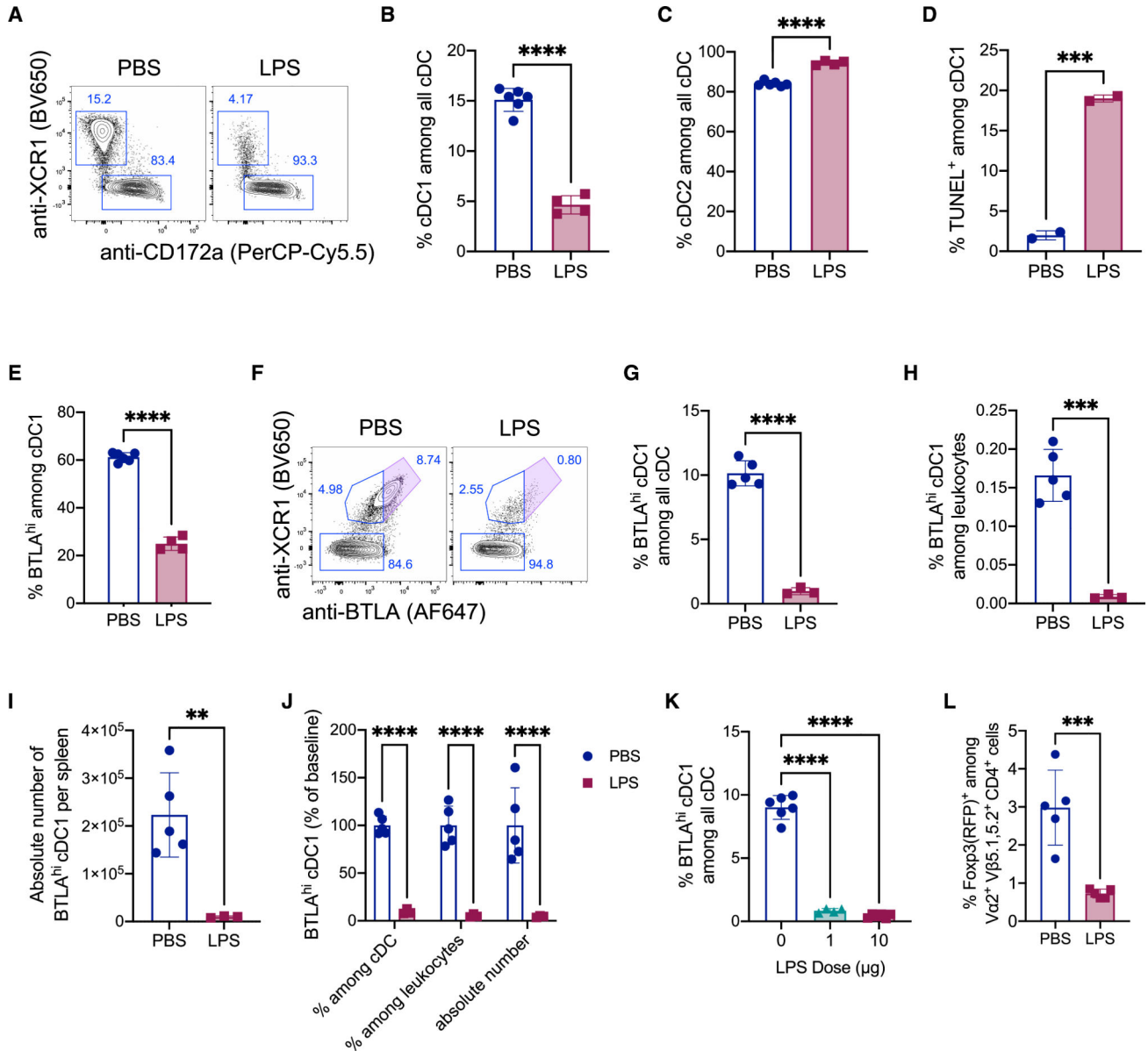


**Figure 1. Ablation of tolerogenic cDCs under pro-inflammatory conditions**

(A–C) Wild-type mice were treated with PBS or LPS (1 μg/mouse) 24 h before analysis of splenocytes by flow cytometry. (A) Plots (representative of multiple independent experiments) show anti-XCR1 and anti-CD172a staining intensity in all cDCs (I-$A^{b+}$$CD11c^{+}$—see gating strategy in Figure S1A). cDC1s are identified as $XCR1^{+}$ ($CD172a^{neg}$), and cDC2s are identified as $CD172a^{+}$($XCR1^{neg}$). Graphs shows percentages of cDC1s (B) or cDC2s (C) among all cDCs in the indicated groups (n = 4–6 mice per group pooled from two independent experiments).

(D) Wild-type mice were treated with PBS or LPS (10 μg/mouse) 6 h before TUNEL analysis of splenocytes by flow cytometry. Graph shows percentages of $TUNEL^{+}$ cells among cDC1s in the indicated groups (n = 2 samples of three mice pooled together per group from two independent experiments).

(E and F) Wild-type mice were treated with PBS or LPS (1 μg/mouse) 24 h before analysis of splenocytes by flow cytometry.

(E) Graph shows percentages of $BTLA^{hi}$ cells among cDC1s (see Figure S1B for the $BTLA^{hi}$ cutoff applied in all experiments; see also F) in the indicated groups (n = 4–6 mice per group pooled from two independent experiments).

(F) Plots (representative of multiple independent experiments) show anti-XCR1 and anti-BTLA staining intensity in all cDCs. The $BTLA^{hi}$ cDC1s are indicated by the purple shaded regions.

(G–J) Wild-type mice were treated with PBS or LPS (10 μg/mouse) 24 h before analysis of splenocytes by flow cytometry (n = 3–5 mice per group pooled from two independent experiments). Graphs show percentages of $BTLA^{hi}$ cDC1s among all cDCs (G) or among all leukocytes (H) or the absolute number of $BTLA^{hi}$ cDC1s per spleen (I) in the indicated groups. (J) Graph shows the percent of baseline (average of the corresponding PBS-treated mice) for $BTLA^{hi}$ cDC1s calculated as a percent among all cDCs, among all leukocytes, or as the absolute number of cells per spleen.

(K) Wild-type mice were treated with PBS or the indicated doses of LPS 24 h before analysis of splenocytes by flow cytometry. Graph shows percentages of $BTLA^{hi}$ cDC1s among all cDCs (in the indicated groups; n = 4–6 mice per group pooled from two independent experiments).

(L) Sorted $Foxp3^{neg}CD25^{neg}$ T cells from OT-II TCR tg *Foxp3*$^{RFP}$ mice were adoptively transferred into wild-type mice that were treated with anti-DEC-OVA only (PBS) or anti-DEC-OVA and 1 μg LPS (LPS) 14 days before analysis of splenocytes by flow cytometry. Graph shows percentages of $Foxp3(RFP)^{+}$ cells among the $V\alpha2^{+}$ $V\beta5.1,5.2^{+}$ $CD4^{+}$ T cells in the indicated groups of recipients (n = 5 mice per group pooled from two independent experiments).

(A and F) Numbers next to outlined regions indicate corresponding percentages. (B–E and G–L) Graphs show mean ± standard deviation (SD). **p < 0.01, ***p < 0.001, and ****p < 0.0001 determined by unpaired two-tailed t test (B–E, G–I, and L), two-way ANOVA with Šídák's multiple comparisons (J), or one-way ANOVA with Tukey's multiple comparisons (K).

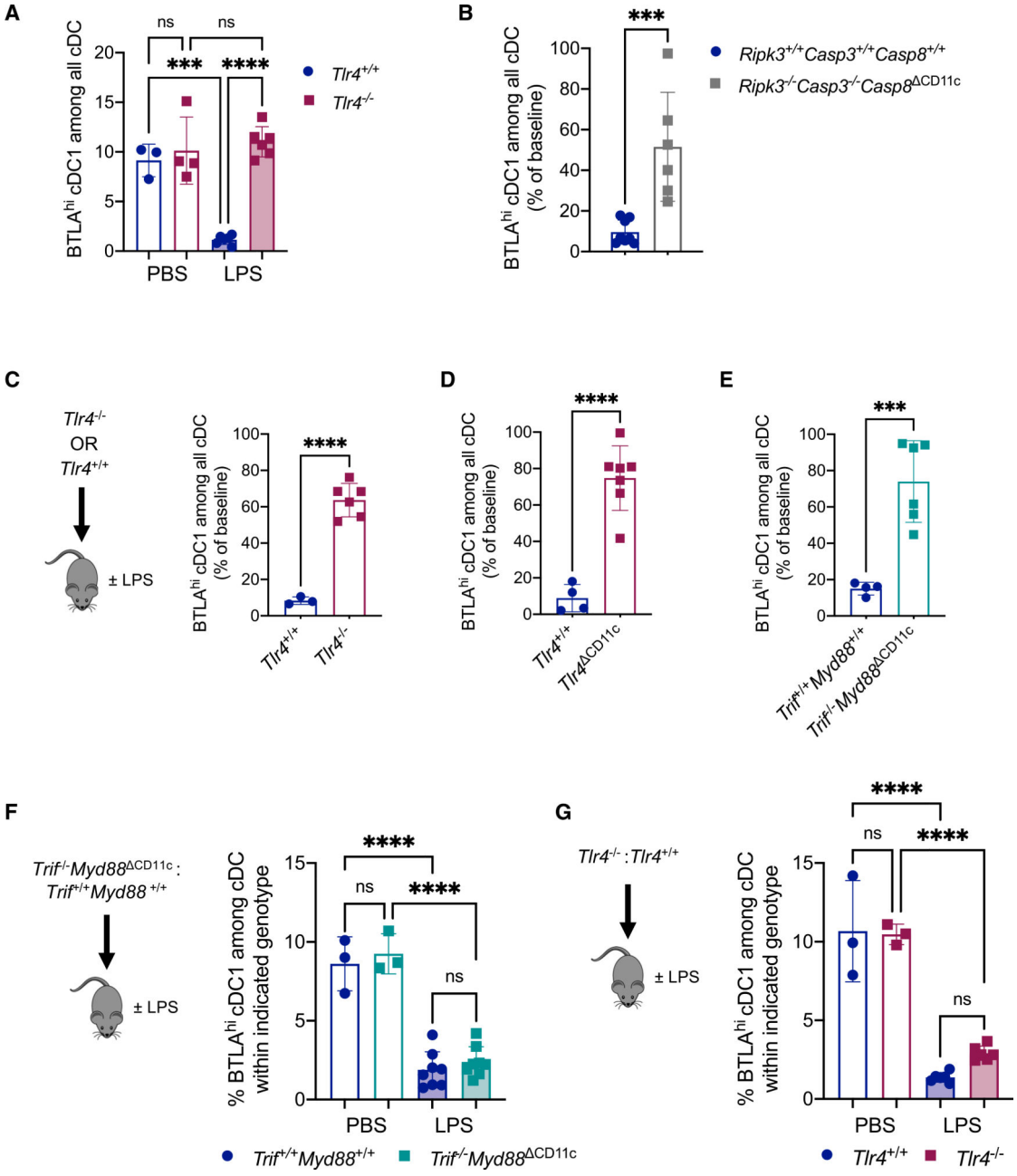


**Figure 2. BTLA$^{hi}$ cDC1s are ablated in *trans***

(A) *Tlr4*$^{+/+}$ and *Tlr4*$^{-/-}$ mice were treated with PBS or LPS (10 μg/mouse) 24 h before analysis of splenocytes by flow cytometry. Graph shows percentages of BTLA$^{hi}$ cDC1s among all cDCs in the indicated groups (n = 3–6 mice per group pooled from three independent experiments).

(B) *Ripk3*$^{+/+}$*Casp3*$^{+/+}$*Casp8*$^{+/+}$ and *Ripk3*$^{-/-}$*Casp3*$^{-/-}$*Casp8*$^{\Delta CD11c}$ mice were treated with PBS or LPS (10 μg/mouse) 24 h before analysis of splenocytes by flow cytometry. Graph shows percentages of BTLA$^{hi}$ cDC1s among all cDCs in LPS-treated mice as a percentage of the baseline (average of the corresponding PBS-treated mice) in the indicated groups (n = 6–8 mice per group pooled from three independent experiments).

(C) Lethally irradiated Tlr4$^{+/+}$ mice were reconstituted with congenically labeled *Tlr4*$^{-/-}$ or *Tlr4*$^{+/+}$ bone marrow (BM). The reconstituted BM chimera mice were treated with PBS or LPS (10 μg/mouse) 24 h before analysis of splenocytes by flow cytometry. (Left) General experimental outline is shown. (Right) Graph shows percentages of BTLA$^{hi}$ cDC1s among all cDCs in LPS-treated mice as a percentage of the baseline (average of the corresponding PBS-treated mice) in the indicated groups (n = 3–6 mice per group pooled from two independent experiments).

(D) *Tlr4*$^{+/+}$ and *Tlr4*$^{\Delta CD11c}$ mice were treated with PBS or LPS (10 μg/mouse) 24 h before analysis of splenocytes by flow cytometry. Graph shows percentages of BTLA$^{hi}$ cDC1s among all cDCs in LPS-treated mice as a percentage of the baseline (average of corresponding PBS-treated mice) in the indicated groups (n = 4–7 mice per group pooled from two independent experiments).

(E) *Trif*$^{+/+}$*Myd88*$^{+/+}$ and *Trif*$^{-/-}$*Myd88*$^{\Delta CD11c}$ mice were treated with PBS or LPS (10 μg/mouse) 24 h before analysis of splenocytes by flow cytometry. Graph shows percentages of BTLA$^{hi}$ cDC1s among all cDCs in LPS-treated mice as a percentage of the baseline (average of corresponding PBS-treated mice) in the indicated groups (n = 4–6 per group pooled from two independent experiments).

(F) Lethally irradiated *Trif*$^{+/+}$*Myd88*$^{+/+}$ mice were reconstituted with a 1:1 mix of congenically labeled *Trif*$^{-/-}$*Myd88*$^{\Delta CD11c}$ and *Trif*$^{+/+}$*Myd88*$^{+/+}$ BM. The reconstituted mixed BM chimera mice were treated with PBS or LPS (10 μg/mouse) 24 h before analysis of splenocytes by flow cytometry. (Left) General experimental outline is shown. (Right) Graph shows percentages of BTLA$^{hi}$ cDC1s among cDCs within the indicated genotype for each treatment (n = 3–8 mice per treatment pooled from two independent experiments).

(G) Lethally irradiated *Tlr4*$^{+/+}$ mice were reconstituted with a 1:1 mix of congenically labeled *Tlr4*$^{-/-}$ and *Tlr4*$^{+/+}$ BM. The reconstituted mixed BM chimera mice were treated with PBS or LPS (10 μg/mouse) 24 h before analysis of splenocytes by flow cytometry. (Left) General experimental outline is shown. (Right) Graph shows percentages of BTLA$^{hi}$ cDC1s among cDCs within the indicated genotype for each treatment (n = 3–6 mice per treatment pooled from two independent experiments).

(A–G) Graphs show mean ± SD. ns, not significant, ***p < 0.001, and ****p < 0.0001 determined by unpaired two-tailed t test (B–E) or one-way ANOVA with Tukey's multiple comparisons (A, F, and G).

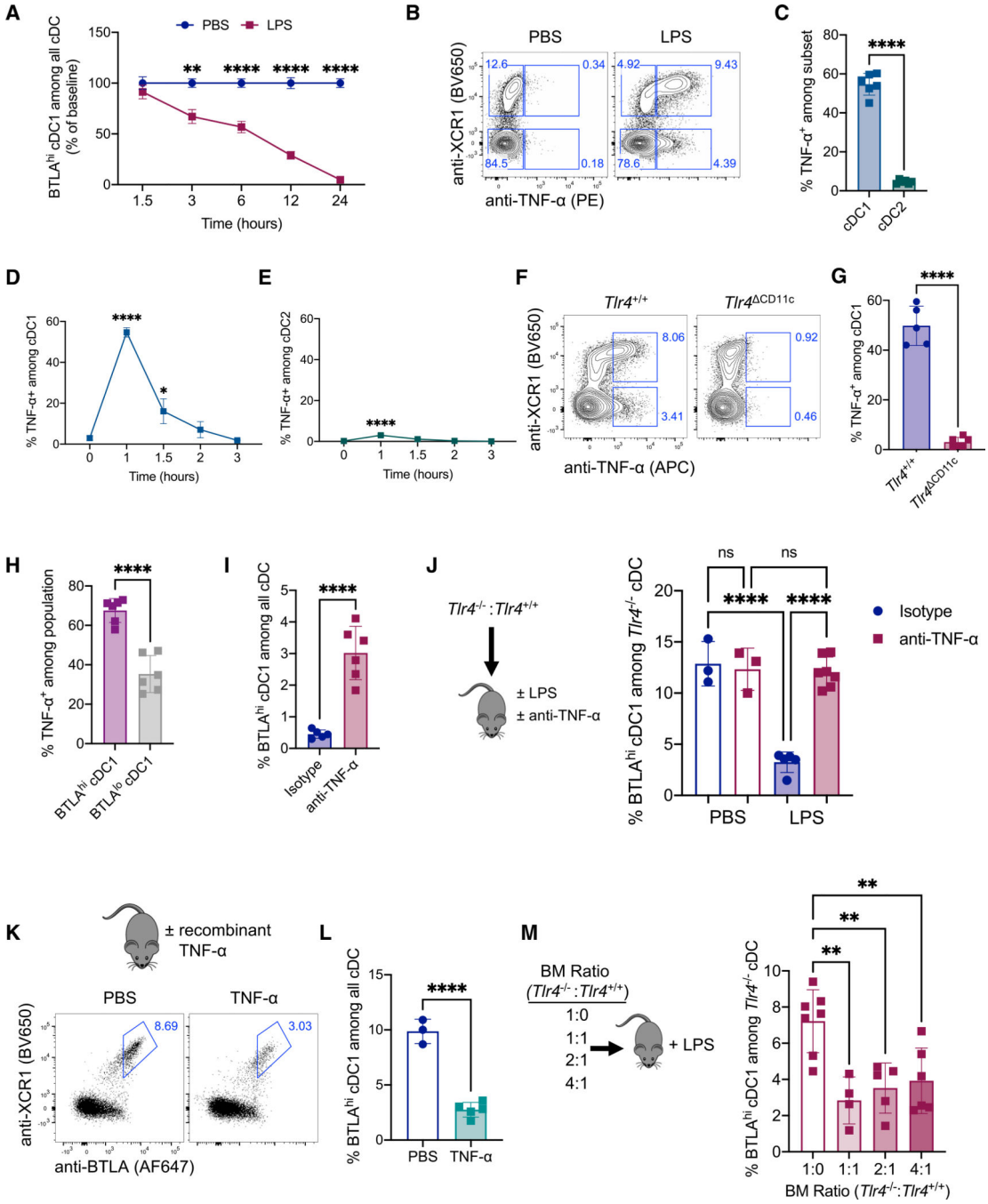


**Figure 3. Rapid production of TNF-α mediates and amplifies the ablation of BTLA$^{hi}$ cDC1s**

(A) Wild-type mice were treated with PBS or LPS (10 μg/mouse) at the indicated time points before analysis of splenocytes by flow cytometry. Graph shows percentages of BTLA$^{hi}$ cDC1s among all cDCs as a percentage of the baseline (average of PBS-treated mice for each time point) in the indicated groups (n = 4–6 mice per group pooled from two independent experiments per time point). Significance is shown for the comparison of PBS and LPS groups at each time point.

(B and C) Wild-type mice were treated with PBS or LPS (10 μg/mouse) 1 h before analysis of splenocytes by flow cytometry.

(B) Plots (representative of multiple independent experiments) show anti-XCR1 and anti-TNF-α intracellular staining intensity in all cDCs.

(C) Graph shows percentages of TNF-$\alpha^+$ cells within the cDC1 (XCR1$^+$ CD172a$^{neg}$) and cDC2 (CD172a$^+$XCR1$^{neg}$) subsets, as indicated, from mice treated with LPS (n = 6 mice pooled from three independent experiments).

(D and E) Wild-type mice were treated with PBS (0 h) or LPS (10 μg/mouse) at the indicated time points before analysis of splenocytes by flow cytometry. Graphs show percentages of TNF-$\alpha^+$ cells within cDC1 (D) or cDC2 (E) subsets for each time point (n = 2–6 mice per group pooled from three independent experiments). Significance is shown for each time point compared with the baseline (0 h).

(F and G) *Tlr4*$^{+/+}$ and *Tlr4*$^{\Delta CD11c}$ were treated with LPS (10 μg) 1 h before analysis of splenocytes by flow cytometry.

(F) Plots (representative of multiple independent experiments) show anti-XCR1 and anti-TNF-α intracellular staining intensity in all cDCs.

(G) Graph shows percentages of TNF-$\alpha^+$ cells within the cDC1 subset in the indicated groups (n = 5–6 mice per group pooled from three independent experiments).

(H) Wild-type mice were treated with PBS or LPS (10 μg/mouse) 1 h before analysis of splenocytes by flow cytometry. Graph shows percentages of TNF-$\alpha^+$ cells within the indicated populations of cDC1s (n = 6 mice pooled from three independent experiments).

(I) Wild-type mice were treated with anti-TNF-α or isotype control antibody as indicated and LPS (10 μg/mouse) 24 h before analysis of splenocytes by flow cytometry. Graph shows percentages of BTLA$^{hi}$ cDC1s among all cDCs in the indicated groups (n = 5–6 mice per group pooled from two independent experiments).

(J) Lethally irradiated *Tlr4*$^{+/+}$ mice were reconstituted with a 1:1 mix of congenically labeled *Tlr4*$^{-/-}$ and *Tlr4*$^{+/+}$ BM. The reconstituted mixed BM chimera mice were treated with anti-TNF-α or isotype control antibody and PBS or LPS (10 μg/mouse) as indicated 24 h before analysis of splenocytes by flow cytometry. (Left) General experimental outline is shown. (Right) Graph shows percentages of BTLA$^{hi}$ cDC1s among *Tlr4*$^{-/-}$ cDCs in the indicated groups (n = 3–7 mice per group pooled from two independent experiments).

(K and L) Wild-type mice were treated with PBS or recombinant mouse TNF-α 24 h before analysis of splenocytes by flow cytometry.

(K) (Top) General experimental outline is shown. (Bottom) Representative plots show anti-XCR1 and anti-BTLA staining intensity in all cDCs.

(L) Graph shows percentages of BTLA$^{hi}$ cDC1s among all cDCs in the indicated groups. Results represent one of two similar experiments (n = 3–5 mice per group).

(M) Lethally irradiated *Tlr4*$^{+/+}$ mice were reconstituted with the indicated ratios of congenically labeled *Tlr4*$^{-/-}$ and *Tlr4*$^{+/+}$ BM. The reconstituted mixed BM chimera mice were treated with LPS (10 μg/mouse) 24 h before analysis of splenocytes by flow cytometry. (Left) General experimental outline is shown. (Right) Graph shows percentages of BTLA$^{hi}$ cDC1s among *Tlr4*$^{-/-}$ cDCs in the indicated groups (n = 4–7 mice per group pooled from two independent experiments).

(B, F, and K) Numbers next to outlined regions indicate corresponding percentages. (A, D, and E) Graphs show mean ± standard error of mean (SEM).

(C, G–J, L, and M) Graphs show mean ± SD. *p < 0.05, **p < 0.01, and ****p < 0.0001 determined by two-way ANOVA with Šídák's multiple comparisons (A), unpaired two-tailed t test (C, G–I, and L), or one-way ANOVA with Tukey's multiple comparisons (D, E, J, and M).

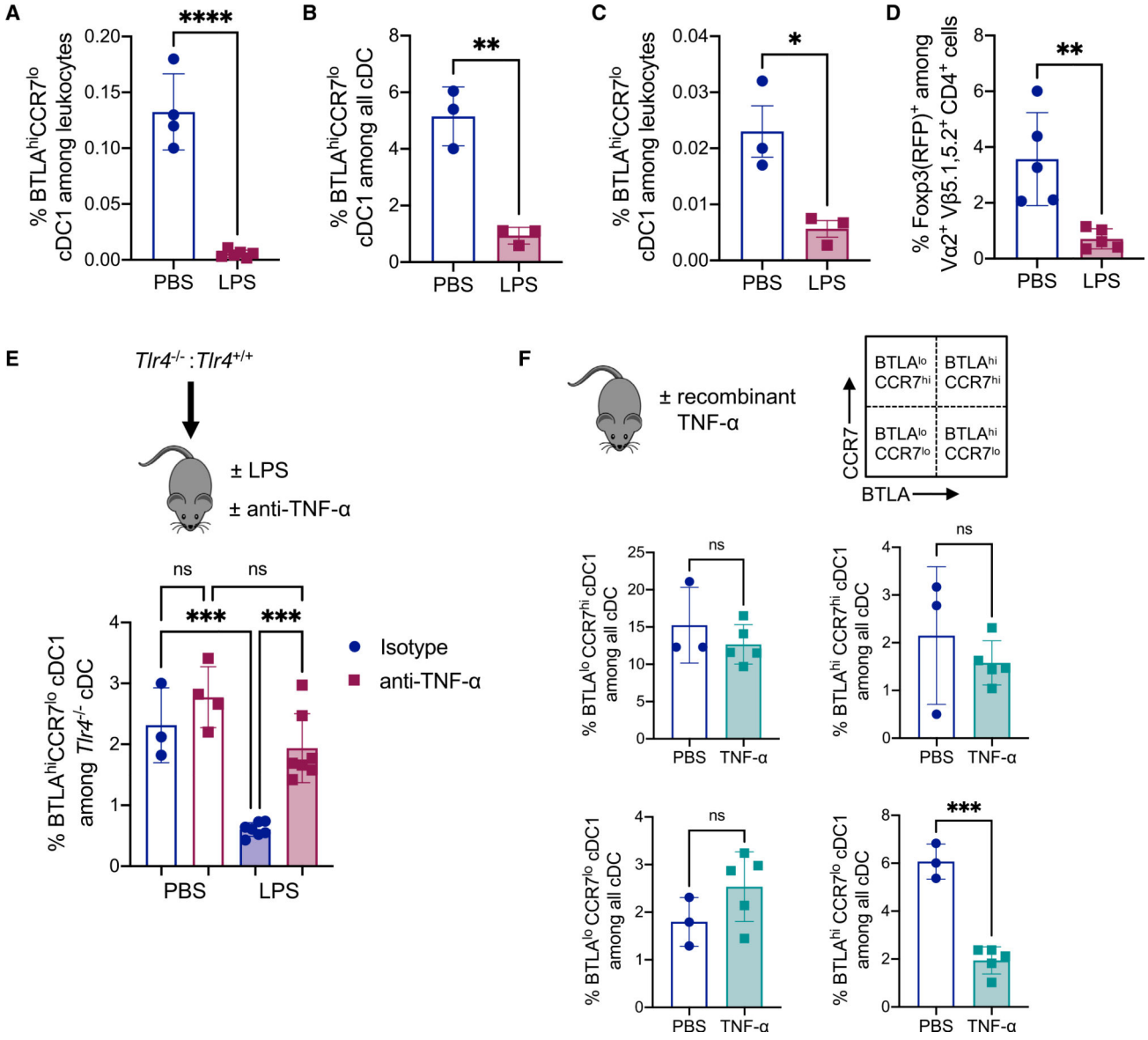


**Figure 4. TNF-α ablates BTLA$^{hi}$(CCR7$^{lo}$) cDC1s throughout peripheral lymphoid organs**

(A) Wild-type mice were treated with PBS or LPS (10 μg/mouse) 24 h before analysis of splenocytes by flow cytometry. Graphs show percentages of BTLA$^{hi}$CCR7$^{lo}$ cDC1s (gated as in Figure S4A) among all leukocytes in the indicated groups (n = 4–6 mice per group pooled from two independent experiments).

(B and C) Wild-type mice were treated with PBS or LPS (10 μg/mouse) 48 h before analysis of peripheral lymph nodes by flow cytometry. Graph shows percentages of BTLA$^{hi}$CCR7$^{lo}$ cDC1s (gated as in Figures S4C and S4D) among all cDCs (B) or among all leukocytes (C) in the indicated groups (n = 3 mice per group). Results represent one of two similar experiments.

(D) Sorted Foxp3$^{neg}$CD25$^{neg}$ T cells from OT-II TCR tg *Foxp3*$^{RFP}$ mice were adoptively transferred into wild-type mice that were treated with anti-DEC-OVA only (PBS) or anti-DEC-OVA and 1 μg LPS (LPS) 14 days before analysis of peripheral lymph nodes by

flow cytometry. Graphs show percentages of Foxp3(RFP)$^+$ cells among Vα2$^+$ Vβ5.1,5.2$^+$ CD4$^+$ T cells in the indicated groups (n = 5 mice per group pooled from two independent experiments).

(E) Lethally irradiated *Tlr4*$^{+/+}$ mice were reconstituted with a 1:1 mix of congenically labeled *Tlr4*$^{-/-}$ and *Tlr4*$^{+/+}$ BM. The reconstituted mixed BM chimera mice were treated with anti-TNF-α or isotype control antibody and PBS or LPS (10 μg/mouse) 48 h before analysis of peripheral lymph nodes by flow cytometry. (Top) General experimental outline is shown. (Bottom) Graph shows percentages of BTLA$^{hi}$CCR7$^{lo}$ cDC1s among *Tlr4*$^{-/-}$ cDCs in the indicated groups (n = 3–7 mice per group pooled from two independent experiments).

(F) Wild-type mice were treated with PBS or recombinant mouse TNF-α 24 h before analysis of peripheral lymph nodes by flow cytometry. (Top) General experimental outline and diagram specifying the populations of cDC1s based on BTLA and CCR7 expression corresponding to populations gated as in Figures S4C and S4D is shown. (Bottom) Graphs show the percentages of the specified populations defined by specific BTLA and CCR7 expression in cDC1s among all cDCs in lymph nodes for the indicated groups. Results represent one of two similar experiments (n = 3–5 mice per group).

(A–F) Graphs show mean ± SD. *$p < 0.05$, **$p < 0.01$, ***$p < 0.001$, and ****$p < 0.0001$ determined by unpaired two-tailed t test (A–D and F) or one-way ANOVA with Tukey's multiple comparisons (E).

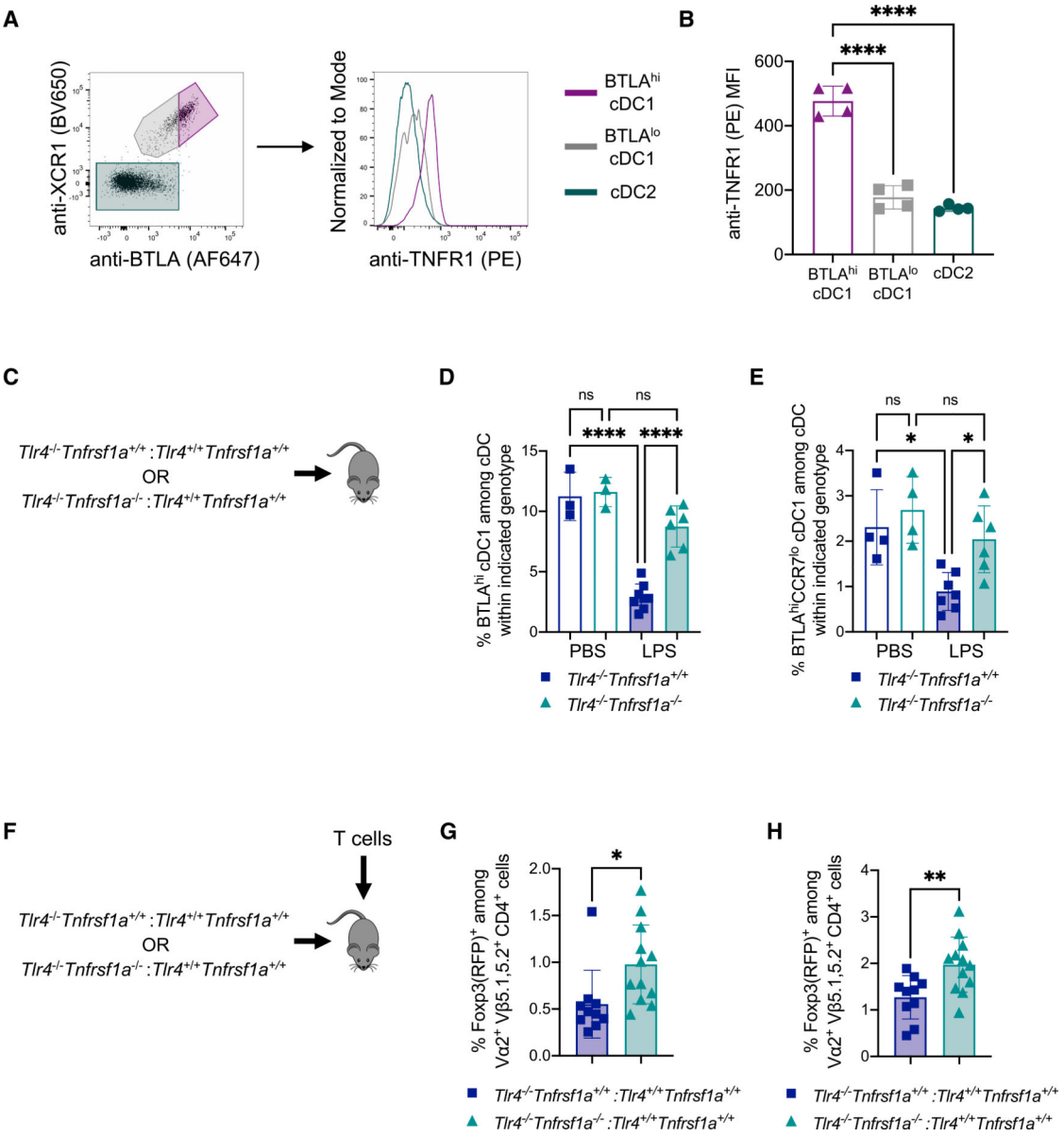


**Figure 5. TNFR1 orchestrates the ablation of tolerogenic BTLA$^{hi}$ cDC1s**

(A and B) Spleens from untreated wild-type mice were analyzed by flow cytometry.

(A) Plot (left) shows anti-XCR1 and anti-BTLA staining intensity in all cDCs. Shaded regions specify gating of populations denoted in the overlaid histograms (right) that show anti-TNFR1 staining intensity of the indicated populations. Results are representative of multiple independent experiments.

(B) Graph shows median fluorescence intensity (MFI) of anti-TNFR1 staining in the indicated populations (gated as in A; n = 4 mice pooled from three independent experiments).

(C–E) Lethally irradiated *Tlr4*$^{+/+}$ *Tnfrsf1a*$^{+/+}$ mice were reconstituted with a 1:1 mix of congenically labeled *Tlr4*$^{-/-}$ *Tnfrsf1a*$^{+/+}$ and *Tlr4*$^{+/+}$ *Tnfrsf1a*$^{+/+}$ or *Tlr4*$^{-/-}$ *Tnfrsf1a*$^{-/-}$ and *Tlr4*$^{+/+}$ *Tnfrsf1a*$^{+/+}$ BM.

(C) General experimental outline for mixed BM chimeras.

(D) Reconstituted mixed BM chimera mice were treated with PBS or LPS (10 μg/mouse) 24 h before analysis of splenocytes by flow cytometry. Graph shows percentages of $BTLA^{hi}$ cDC1s among cDCs within the indicated genotype for each treatment (n = 3–8 mice per group pooled from two independent experiments).

(E) Reconstituted mixed BM chimera mice were treated with PBS or LPS (10 μg/mouse) 48 h before analysis of peripheral lymph nodes by flow cytometry. Graph shows percentages of $BTLA^{hi}CCR7^{lo}$ cDC1s among cDCs within the indicated genotype for each treatment (n = 4–7 mice per group pooled from three independent experiments).

(F–H) Lethally irradiated *Tlr4*$^{+/+}$ *Tnfrsf1a*$^{+/+}$ mice were reconstituted with a 2:1 mix of congenically labeled *Tlr4*$^{-/-}$ *Tnfrsf1a*$^{+/+}$ and *Tlr4*$^{+/+}$ *Tnfrsf1a*$^{+/+}$ or *Tlr4*$^{-/-}$ *Tnfrsf1a*$^{-/-}$ and *Tlr4*$^{+/+}$ *Tnfrsf1a*$^{+/+}$ BM. Sorted $Foxp3^{neg}CD25^{neg}$ T cells from OT-II TCR tg *Foxp3*$^{RFP}$ mice were adoptively transferred into the reconstituted mixed BM chimera mice that were treated with anti-DEC-OVA and LPS (10 μg/mouse) 14 to 15 days before analysis of spleens and peripheral lymph nodes by flow cytometry.

(F) General experimental outline for adoptive transfers into reconstituted mixed BM chimeras.

(G and H) Graphs show percentages of $Foxp3(RFP)^{+}$ cells among $V\alpha2^{+}$ $V\beta5.1,5.2^{+}$ $CD4^{+}$ T cells in the indicated groups of recipients among splenocytes (G) or lymph node cells (H) (n = 10–12 mice per group pooled from three independent experiments).

(B, D, E, G, and H) Graphs show mean ± SD. *p < 0.05, **p < 0.01, and ****p < 0.0001 determined by one-way ANOVA with Tukey's multiple comparisons (B, D, and E) or unpaired two-tailed t test (G and H).

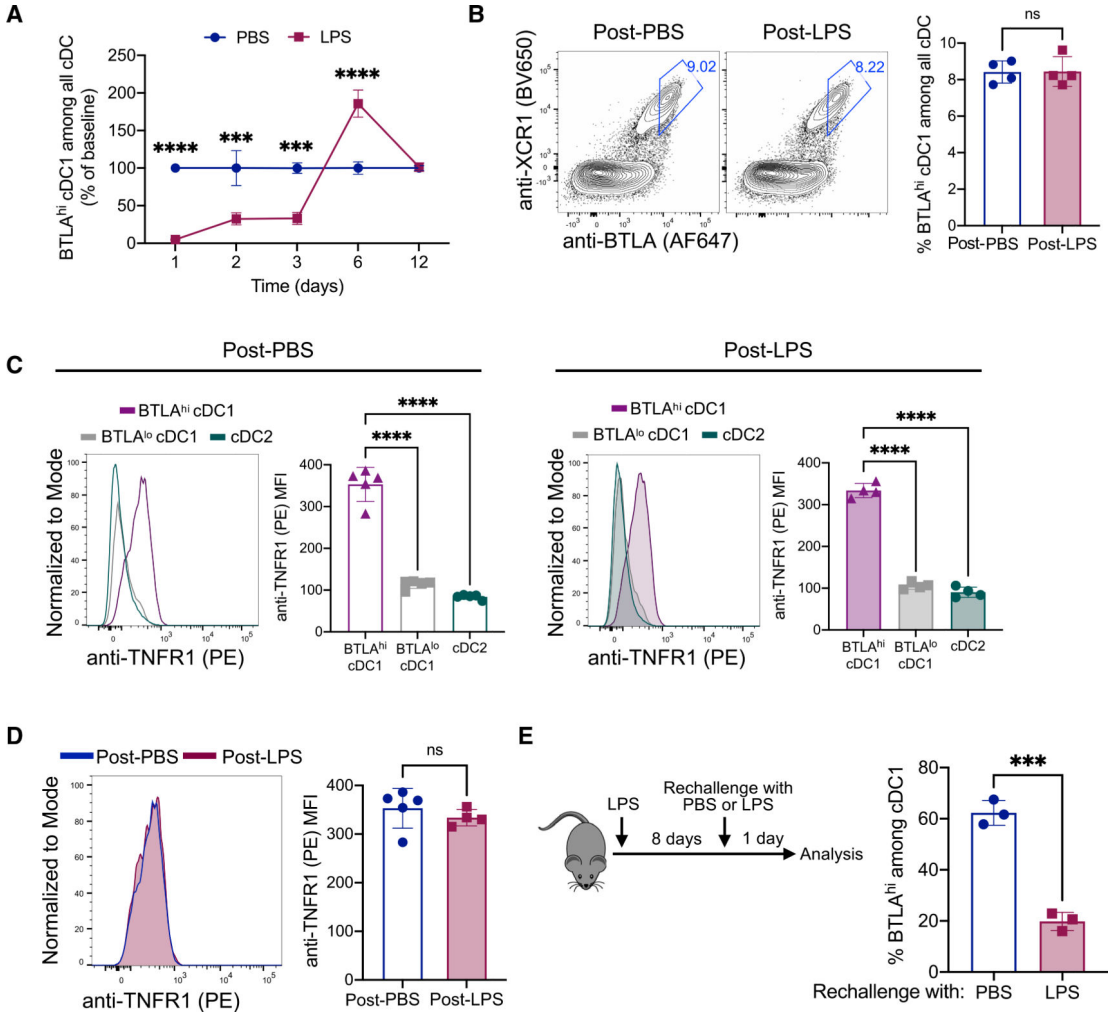


**Figure 6. Return to the homeostatic baseline by BTLA$^{hi}$ cDC1s**

(A) Wild-type mice were treated with PBS or LPS (10 μg/mouse) at the indicated time points before analysis of splenocytes by flow cytometry. Graph shows percentages of BTLA$^{hi}$ cDC1s among all cDCs as a percentage of the baseline (average of PBS-treated mice for each time point) at the indicated time points (n = 4–7 mice per group pooled from two independent experiments per time point). Significance is shown for the comparison of PBS and LPS groups at each time point.

(B) Wild-type mice were treated with PBS or LPS (10 μg/mouse) 12 days before analysis of splenocytes by flow cytometry. Plots (representative of multiple independent experiments) show anti-XCR1 and anti-BTLA staining intensity in all cDCs. Numbers next to outlined regions indicate corresponding percentages. Graph shows percentages of BTLA$^{hi}$ cDC1s among all cDCs in the indicated groups (n = 4 mice per group pooled from two independent experiments).

(C and D) Wild-type mice were treated with PBS or LPS (10 μg/mouse) 9 days before analysis of splenocytes by flow cytometry.

(C) Overlaid histograms (representative of two independent experiments) show anti-TNFR1 staining intensity of the indicated populations (gated as in Figure 5A) from PBS-treated

mice and 9 days post-LPS treatment. Corresponding graphs show MFI of anti-TNFR1 staining in the indicated populations for the indicated treatments (n = 4–5 mice per group pooled from two independent experiments).

(D) Overlaid histogram (representative of two independent experiments) shows anti-TNFR1 staining intensity of $BTLA^{hi}$ cDC1s from PBS-treated mice and 9 days post-LPS treatment as indicated. Corresponding graph shows MFI of anti-TNFR1 staining in $BTLA^{hi}$ cDC1s for the indicated treatments (n = 4–5 mice per group pooled from two independent experiments).

(E) Wild-type mice were treated with PBS or LPS (10 μg/mouse) 8 days before re-challenge with either PBS or LPS (10 μg/mouse). Splenocytes were analyzed by flow cytometry 1 day later. (Left) General experimental outline is shown. (Right) Graph shows percentages of $BTLA^{hi}$ cells among cDC1s in the indicated groups (n = 3 mice per group).

(A) Graph shows mean ± SEM. (B–E) Graphs show mean ± SD. ***$p < 0.001$ and ****$p < 0.0001$ determined by two-way ANOVA with Šídák's multiple comparisons (A), one-way ANOVA with Tukey's multiple comparisons (C), or unpaired two-tailed t test (B, D, and E).

## KEY RESOURCES TABLE

| REAGENT or RESOURCE | SOURCE | IDENTIFIER |
|---|---|---|
| Antibodies | | |
| Anti-Mouse CD3ε, Clone: 145-2C11 | BioLegend | Cat#:100308; RRID: AB_312673 |
| Anti-Mouse CD3ε, Clone: 145-2C11 | BioLegend | Cat#:100310; RRID: AB_312675 |
| Anti-Mouse CD3ε, Clone: 145-2C11 | BioLegend | Cat#: 100304; RRID: AB_312669 |
| Anti-Mouse CD4, Clone GK1.5 | BioLegend | Cat#: 100447; RRID: AB_2564586 |
| Anti-Mouse CD8α, Clone: 53-6.7 | BioLegend | Cat#:100704; RRID: AB_312743 |
| Anti-Mouse CD11b, Clone: M1/70 | BioLegend | Cat#:101204; RRID: AB_312787 |
| Anti-Mouse CD11c, Clone: N418 | BioLegend | Cat#:117304; RRID: AB_313773 |
| Anti-Mouse CD11c, Clone: N418 | BioLegend | Cat#:117336; RRID: AB_2565268 |
| Anti-Mouse CD120a / TNFR Type I/p55, Clone: 55R-286 | BioLegend | Cat#:113003; RRID: AB_313532 |
| Anti-Mouse CD16/32, Clone: 2.4G2 | ATCC | Produced in-house from hybridomas obtained from ATCC (Cat#: HB-197™; RRID: CVCL_9148) |
| Anti-Mouse CD172a, Clone: P84 | BioLegend | Cat#:144010; RRID: AB_2563548 |
| Anti-Mouse CD19, Clone: 6D5 | BioLegend | Cat#:115508; RRID: AB_313643 |
| Anti-Mouse CD19, Clone: 6D5 | BioLegend | Cat#:115510; RRID: AB_313645 |
| Anti-Mouse CD197 (CCR7), Clone: 4B12 | BioLegend | Cat#:120105; RRID: AB_389357 |
| Anti-Mouse CD197 (CCR7), Clone: 4B12 | BioLegend | Cat#:120110; RRID: AB_492841 |
| Anti-Mouse CD25, Clone: PC61 | BioLegend | Cat#:102030; RRID: AB_893288 |
| Anti-Mouse CD272 (BTLA), Clone: 6A6 | BioLegend | Cat#:139106; RRID: AB_10613297 |
| Anti-Mouse CD45, Clone: 30-F11 | BioLegend | Cat#: 103128; RRID: AB_493715 |
| Anti-Mouse CD45R/B220, Clone: RA3-6B2 | BioLegend | Cat#:103208; RRID: AB_312993 |
| Anti-Mouse CD45R/B220, Clone: RA3-6B2 | BioLegend | Cat#:103210; RRID: AB_312995 |
| Anti-Mouse CD45R/B220, Clone: RA3-6B2 | BioLegend | Cat#:103204; RRID: AB_312989 |
| Anti-Mouse CD45.1, Clone: A20 | BioLegend | Cat#:110714; RRID: AB_313503 |
| Anti-Mouse CD45.1, Clone: A20 | BioLegend | Cat#:110706; RRID: AB_313495 |
| Anti-Mouse CD45.1, Clone: A20 | BioLegend | Cat#: 110722; RRID: AB_492866 |
| Anti-Mouse CD45.2, Clone: 104 | BioLegend | Cat#:109830; RRID: AB_1186098 |
| Anti-Mouse CD45.2, Clone: 104 | BioLegend | Cat#:109814; RRID: AB_389211 |
| Anti-Mouse CD49b, Clone: DX5 | BioLegend | Cat#:108904; RRID: AB_313411 |
| Anti-Mouse CD64, Clone: X54-5/7.1 | BioLegend | Cat#:139323; RRID: AB_2629778 |
| Anti-Mouse CD86, Clone GL-1 | BioLegend | Cat#: 105007; RRID: AB_313150 |
| Anti-Mouse F4/80, Clone: BM8 | BioLegend | Cat#:123118; RRID: AB_893477 |
| Anti-Mouse I-Ab, Clone: AF6-120.1 | BioLegend | Cat#:116422; RRID: AB_10613473 |
| Anti-Mouse NK1.1, Clone: PK136 | BioLegend | Cat#:108707; RRID: AB_313394 |
| Anti-Mouse NK1.1, Clone: PK136 | BioLegend | Cat#:108716; RRID: AB_493590 |
| Anti-Mouse TCR $V_{\alpha}2$, Clone: B20.1 | BioLegend | Cat#: 127824; RRID: AB_2814019 |
| Anti-Mouse TCR $V_{\beta}5.1/5.2$, Clone: MR9-4 | BioLegend | Cat#:139507; RRID: AB_2566020 |
| Anti-Mouse TNF-α, Clone: MP6-XT22 | BioLegend | Cat#: 506307; RRID: AB_315428 |
| Anti-Mouse TNF-α, Clone: MP6-XT22 | BioLegend | Cat#:506305; RRID: AB_315426 |
| Anti-Mouse XCR1, Clone: ZET | BioLegend | Cat#:148220; RRID: AB_2566410 |

| REAGENT or RESOURCE | SOURCE | IDENTIFIER |
|---|---|---|
| Armenian Hamster IgG Isotype Ctrl Antibody, Clone HTK888 | Biolegend | Cat#: 400924 |
| InVivoMab Anti-Horseradish Peroxidase (Rat IgG1 Isotype Control), Clone: HRPN | BioXcell | Cat#:BE0088; RRID: AB_1107775 |
| InVivoMab Anti-Mouse TNF-α, Clone: XT3.11 | BioXcell | Cat#:BE0058; RRID: AB_1107764 |
| Chemicals, peptides, and recombinant proteins | | |
| 2-Mercaptoethanol | Gibco | Cat#: 21985-023 |
| Dulbecco's Phosphate Buffered Saline | Hyclone | Cat#: SH30028FS |
| Hanks' Balanced Salt Solution | Gibco | Cat#: 14175095 |
| HEPES | Gibco | Cat#: 15630-080 |
| Penicillin-Streptomycin | Gibco | Cat#: 15140-122 |
| RPMI 1640 medium | Hyclone | Cat#: SH30027FS |
| Sodium Pyruvate | Gibco | Cat#: 11360-070 |
| Recombinant Mouse TNF-α (carrier-free) | Biolegend | Cat#: 575204 |
| Critical commercial assays | | |
| APO-BrdU™ TUNEL Kit | BD | Cat#: 556405 |
| BD Cytofix/Cytoperm™ Fixation/Permeabilization Kit | BD | Cat#: 554714 |
| Zombie Aqua™ Fixable Viability Kit | BioLegend | Cat#: 423102 |
| Experimental models: Cell lines | | |
| Cell Line: Expi293F™ | ThermoFisher | Cat#: A14527; RRID: CVCL_D615 |
| Experimental models: Organisms/strains | | |
| Mouse: C57BL/6J | Jackson Laboratory | Stock# 000664 |
| Mouse: B6.SJL-Ptprc$^{a}$ Pepc$^{b}$/BoyJ | Jackson Laboratory | Stock# 002014 |
| Mouse: *Btla*$^{-/-}$ | Jackson Laboratory | Stock# 006353; Sedy et al., 2005 |
| Mouse: *Casp3*$^{-/-}$ | Jackson Laboratory | Stock# 006233; Kuida et al., 1996 |
| Mouse: *Casp8*$^{fl/fl}$ | Jackson Laboratory | Stock# 027002; Beisner et al., 2005 |
| Mouse: CD19-Cre | Jackson Laboratory | Stock# 006785; Rickert et al., 1997 |
| Mouse: B6.MRL-Fas$^{lpr}$/J | Jackson Laboratory | Stock# 000482; Watanabe-Fukunaga et al., 1992 |
| Mouse: *Foxp3*$^{RFP}$ reporter | Jackson Laboratory | Stock# 008374; Wan and Flavell, 2005 |
| Mouse: *Ifnar1*$^{-/-}$ | Jackson Laboratory | Stock# 032045-JAX; Müller et al., 1994 |
| Mouse: *Ifnar1*$^{-/-}$ | Jackson Laboratory | Stock# 028288; Hayashi et al., 2002; Prigge et al., 2015 |
| Mouse: *Itgax*-Cre | Jackson Laboratory | Stock# 008068; Caton et al., 2007 |
| Mouse: LysM-Cre | Jackson Laboratory | Stock# 004781; Clausen et al., 1999 |
| Mouse: *Myd88*$^{fl/fl}$ | Jackson Laboratory | Stock# 008888; Hou et al., 2008 |
| Mouse: OTII TCR tg | Jackson Laboratory | Stock# 004194; Barnden et al., 1998 |
| Mouse: *Ripk3*$^{-/-}$ | Jackson Laboratory | Stock# 025738; Newton et al., 2004 |
| Mouse: *Ticam1*$^{-/-}$ (*Trif*$^{-/-}$) | Jackson Laboratory | Stock# 005037; Hoebe et al., 2003 |

| REAGENT or RESOURCE | SOURCE | IDENTIFIER |
|---|---|---|
| Mouse: *Tlr4*$^{-/-}$ | Jackson Laboratory | Stock# 029015; Hayashi et al., 2002; McAlees et al., 2015 |
| Mouse: *Tlr4*$^{fl/fl}$ | Jackson Laboratory | Stock# 024872; McAlees et al., 2015 |
| Mouse: *Tnfrsf1a*$^{-/-}$ | Jackson Laboratory | Stock# 003242; Peschon et al., 1998 |
| Software and algorithms | | |
| FlowJo 10 | FlowJo, LLC | https://www.flowjo.com; RRID: SCR_008520 |
| GraphPad Prism | GraphPad Software | https://www.graphpad.com; RRID: SCR_002798 |
| Other | | |
| BenchMark Fetal Bovine Serum | Gemini Bio-Products | Cat#: 100-106 |
| Roche Collagenase D | MilliporeSigma | Cat#: 11088882001 |
| Ultrapure LPS, E. coli 0111:B4 (LPS-EB Ultrapure) | InvivoGen | Cat#: tlrl-3pelps |
| Protein G Sepharose Beads | GE Healthcare | Cat#: 17061801 |
| Streptavidin MicroBeads | Miltenyi | Cat#: 130-048-101 |
| LS Columns | Miltenyi | Cat#: 130-042-401 |